**Annotation of glycolysis, gluconeogenesis, and trehaloneogenesis pathways provide insight into carbohydrate metabolism in the Asian citrus psyllid.**

Blessy Tamayo, Kyle Kercher, Chad Vosburg, Crissy Massimino, Margaryta R. Jernigan, Denisse L. Hasan, Douglas Harper, Anuja Mathew, Samuel Adkins, Teresa Shippy, Prashant S. Hosmani, Mirella Flores-Gonzalez, Naftali Panitz, Lukas A. Mueller, Wayne B. Hunter, Joshua B. Benoit, Susan J. Brown, Tom D'Elia and Surya Saha

1 Indian River State College, Fort Pierce, FL 34981, USA 2 Division of Biology, Kansas State University, Manhattan, KS 66506, USA 3 Boyce Thompson Institute, Ithaca, NY 14853, USA 4 USDA-ARS, US Horticultural Research Laboratory, Fort Pierce, FL 34945, USA 5 Department of Biological Sciences, University of Cincinnati, Cincinnati, OH 45221, USA 6 Animal and Comparative Biomedical Sciences, University of Arizona, Tucson, AZ 85721, USA

**Keywords**: *Diaphorina citri*, glycolysis, gluconeogenesis, trehaloneogenesis, genome annotation

## Abstract

Citrus greening disease is caused by the pathogen *Candidatus* Liberibacter asiaticus, which is transmitted by the Asian citrus psyllid, *Diaphorina citri*. There is no curative treatment or significant prevention mechanism for this detrimental disease that causes continued economic losses from reduced citrus production. A high quality genome of *D. citri* is being manually annotated to provide accurate gene models required to identify novel control targets and increase understanding of this pest. Here, we annotated genes involved in glycolysis, gluconeogenesis, and trehaloneogenesis in the *D. citri* genome, as these are core metabolic pathways and suppression could reduce this pest. Specifically, twenty-five genes were identified and annotated in the glycolysis and gluconeogenesis pathways and seven genes for the trehaloneogenesis pathway. Comparative analysis showed that the glycolysis genes in *D. citri* are highly conserved compared to orthologs in other insect systems, but copy numbers vary in *D. citri*. Expression levels of the annotated gene models were analyzed and several enzymes in

the glycolysis pathway showed high expression in the thorax. This is consistent with the primary use of glucose by flight muscles located in the thorax. A few of the genes annotated in *D. citri* have been targeted for gene knockdown as a proof of concept, for RNAi therapeutics. Thus, manual annotation of these core metabolic pathways provides accurate genomic foundations for developing gene-targeting therapeutics to reduce *D. citri*.

**Research Area:** Genetics and Genomics

**Classifications:** Animal Genetics, Bioinformatics

## Data Description

### Introduction

Huanglongbing, HLB, or citrus greening disease is the biggest global threat to the citrus industry throughout the world [1]. The phloem-limited bacterial pathogen *Candidatus* Liberibacter asiaticus (*C*Las) is the causative agent of HLB. Upon infection of a citrus tree, HLB causes development of small, bitter fruits, loss of tree vigor, fruit drop, and ultimately tree decline and death [1]; [2]; [3], [4]. This bacterium is transmitted by the psyllid vector, *D. citri*, when feeding on citrus [5]; [6]. Pesticide application to eliminate *D. citri* has not been successful and no cure for HLB exists [7]; [8]. To develop new psyllid control strategies, The International Psyllid Genome Consortium was established in 2009 [9] to provide the genome, transcriptome resources, and an Official Gene Set of *D. citri* [10]; [11]. A recent, nearly complete genome with significantly improved gene accuracy has been generated, providing a significant data set for the establishment of gene-targeted strategies to suppress psyllid populations (*opensource*: Diaci_v3.0,

www.citrusgreening.org) [USDA-NIFA grant 2015-70016-23028]. As part of this genome project, we conducted manual annotation of genes in critical pathways to provide the quality gene models required for designing molecular therapeutics such as RNA interference (RNAi) [12]; [13]; [14]; [15]; [16]; [17]; [18]; [19]; [20], antisense oligonucleotides (ASO) [21]; [15]; [19], and gene editing (CRISPR) [22]; [23]. Here, we examined *D. citri* orthologs associated with the critical metabolic pathways glycolysis, gluconeogenesis, and trehaloneogenesis.

**Context**

A community-driven annotation strategy was used to identify and characterize the genes encoding enzymes involved in glycolysis, gluconeogenesis, and trehaloneogenesis (Fig. 1). Glycolysis is a major metabolic pathway that plays a vital role in core energy processing reactions, and as a source of metabolites for other biochemical processes. For insects, there is a high utilization of glucose in flight muscle located in the thorax [24]. As a result, the activities of glycolytic enzymes are increased in insect flight muscle compared to vertebrate muscle tissue [25]. Gluconeogenesis is essential in insects to maintain sugar homeostasis and serves as the initial step towards the generation of glucose disaccharide, also known as trehalose. Trehalose is the main circulating sugar in the insect hemolymph [26]; [27]; [28]. In trehaloneogenesis, glucose-6-phosphate is converted into trehalose by trehalose 6 phosphate synthase (TPS). Trehalase enzymes then degrade trehalose into two glucose molecules [29]. Genes involved in psyllid glycolysis, gluconeogenesis, and trehaloneogenesis have been targeted by several RNAi studies (Appendix Table 1) as a promising avenue for psyllid

population suppression. In particular, one proof of concept experiment targeting trehalase has led to the release of the first RNAi patent to control psyllid populations [30]. RNAi, as a biopesticide, and strategies for delivery and applications to target insect pests and viral pathogens have been thoroughly reviewed [31]; [32]; [33]; [34]; [35].

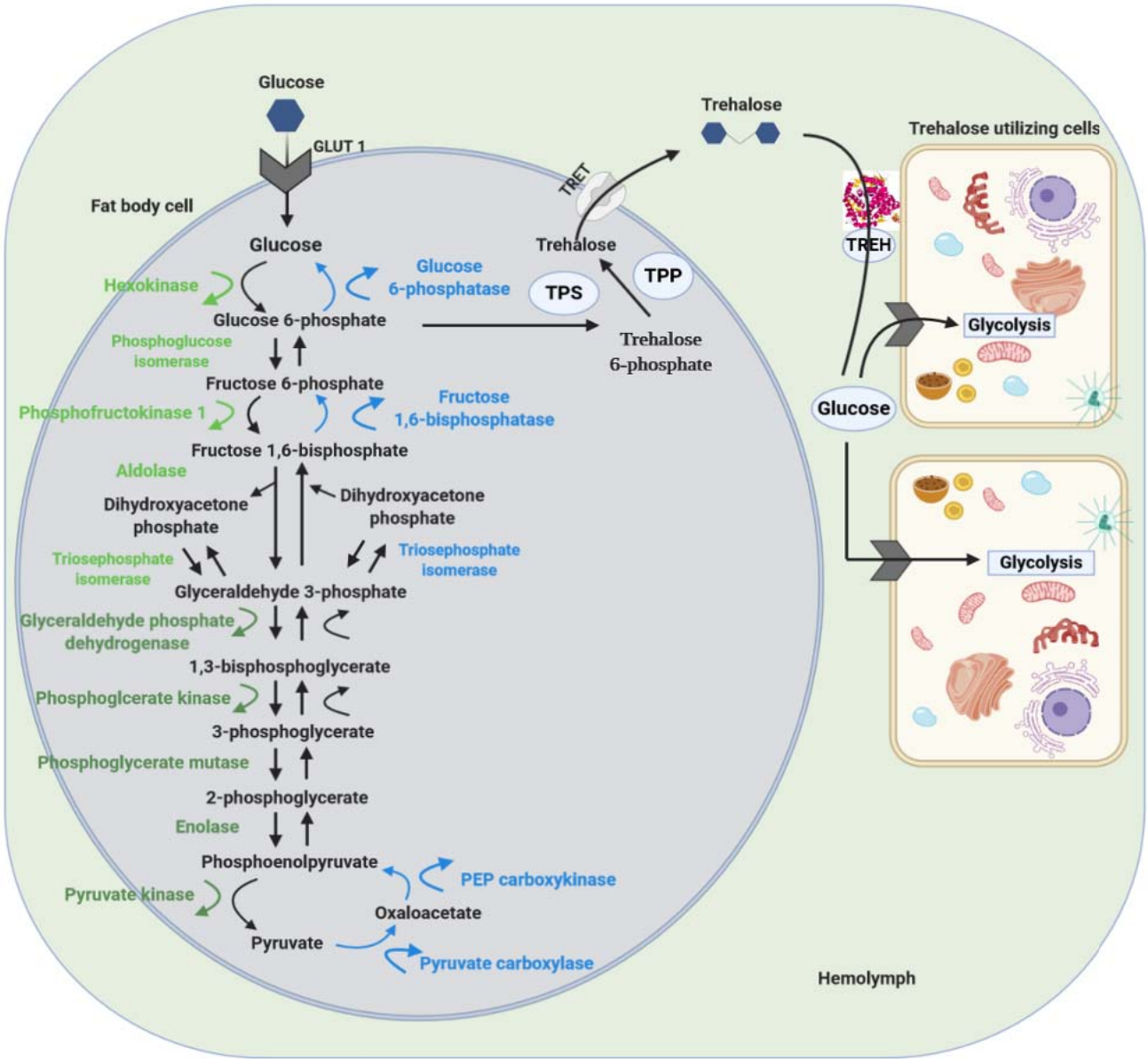


**Figure 1: Overview of Glycolysis, Gluconeogenesis, and Trehaloneogenesis Pathway Image.**

The pathway image shows the enzymes that produce and utilize glucose and trehalose in insects [36]. The glycolysis pathway consists of ten enzymes that convert glucose into pyruvate as the final product. These are divided into the energy investment phase (light green) and the energy production phase (dark green). The gluconeogenesis pathway consists of eight enzymes (blue) with three being unique to the pathway that bypasses the irreversible reactions in glycolysis to convert non-carbohydrate molecules into glucose. The trehaloneogenesis pathway consists of three enzymes which are *Trehalose-6-phosphate synthase* (*TPS*), *Trehalose-6-phosphate phosphatase* (*TPP*), and *Trehalase* (*TREH*), as well as *Trehalose transporters* (*TRET*) and *Glucose transporters* (*GLUT 1*). Image was adapted from a diagram in [37], and was created with BioRender.com.

**Methods**

The *D. citri* genome was manually annotated through a collaborative community [11] driven strategy with an undergraduate focus that allows specific students to focus on main gene sets [38]. Orthologous protein sequences for the glycolysis, gluconeogenesis, and trehaloneogenesis pathways were obtained from the National Center for Biotechnology Information (NCBI) protein database [39] and were used to BLAST the *D. citri* MCOT (Maker (RRID:SCR_005309), Cufflinks (RRID:SCR_014597), Oases (RRID:SCR_011896), and Trinity (RRID:SCR_013048)) protein database to find predicted protein models [36]. The MCOT predicted protein models were used for searching the *D. citri* genomes (version 2.0 and 3.0) [38]. Regions of high sequence identity were manually curated in Apollo version 2.1.0 (RRID:SCR_001936) using *de*

*novo* transcriptome, MCOT gene predictions, RNA-seq, Iso-seq, and ortholog data to support and evaluate gene structure (Appendix Table 2). The curated gene models were compared to other orthologous sequences, such as hemipterans, available through NCBI for accuracy. A more detailed description of the annotation workflow is available (Fig. 2) [40].

Neighbor-joining phylogenetic tree of the annotated *hexokinase* gene models in *D. citri* and orthologous sequences were created with MEGA version 7 (RRID:SCR_000667) using the MUSCLE (RRID:SCR_011812) multiple sequence alignment with p-distance for determining branch length and 1,000 bootstrap replicates [41].

Expression levels of the carbohydrate metabolism genes throughout different life stages (egg, nymph, and adult) in *C*Las infected and uninfected *D. citri* insects were collected from the Citrus Greening Expression Network (CGEN) [36] and visualized using Excel (RRID:SCR_016137) and the pheatmap package in R. (RRID:SCR:_016418).

Dec 16, 2020

Annotating genes in Diaphorina citri genome version 3

Teresa Shippy[1], S Miller[2], C Massimino[3], C Vosburg [Indian River State College[4]. PS Hosmani[5]. M Flores-Gonzalez[5]. LA...
[1]Kansas State University, [2]Kansas State University, Allen County Community College. [3]Indian River State College....

Figure 2: Protocols.io protocol for psyllid genome curation [40].

**Data Validation and Quality Control**

The characterization of the carbohydrate metabolism pathways in *D. citri* is separated into four sections: the energy investment phase of glycolysis, the energy production

phase of glycolysis, gluconeogenesis, and trehaloneogenesis. The enzymes involved in the breakdown and synthesis of glucose and trehalose were annotated in version 3.0 of the *D. citri* genome [42]. The following genes in the energy investment phase: *hexokinase* (*HK*), *phosphoglucose isomerase* (*PGI*), *phosphofructokinase* (*PFK*), *Fructose-bisphosphate aldolase* (*aldolase*), *triosephosphate isomerase* (*TPI*), and in the energy production phase: *glyceraldehyde phosphate dehydrogenase* (*GAPDH*), *phosphoglycerate kinase* (*PGK*), *phosphoglycerate mutase* (*PGAM*), *enolase*, and *pyruvate kinase* (*PYK*) were annotated. The annotated genes for gluconeogenesis are *pyruvate carboxylase* (*PC*), *phosphoenolpyruvate carboxykinase* (*PEPCK*), and *fructose 1,6-bisphosphatase* (*FBPase*). In trehaloneogenesis, *trehalose transporter 1* (*TRET-1*) and *2* (*TRET-2*), *glucose transporter 1* (*GLUT-1*), and two gene models of both *trehalose-6-phosphate synthase* (*TPS*) and *trehalase* (*TREH*) were annotated. Gene expression data sets in CGEN were analyzed for potential differences, as expression patterns can provide insight into potential RNAi target candidates for molecular therapeutics (Appendix Table 1).

Orthologous sequences from related insects and information about conserved motifs or domains were used to determine the final annotation. We used proteins from *Drosophila melanogaster* (*Dm*) [43], *Tribolium castaneum* (*Tc*) [44], *Apis mellifera* (*Am*) [45], *Acyrthosiphon pisum* (*Ap*) [46], *Nilaparvata lugens* (*Nl*) [47]; [48], *Halyomorpha halys* (*Hh*) [49].

**Energy investment phase of glycolysis**

*HK* catalyzes the first step in glycolysis, utilizing ATP to phosphorylate glucose creating glucose-6-phosphate. Most insects have multiple *HK* genes and three copies of *HK* are present in the *D. citri* genome (Fig. 3, Table 3 and Appendix Table 2). In insect flight muscles, *HK* activity is inhibited by its product, glucose-6-phosphate, to initiate flight muscle activity [50]. *Drosophila melanogaster* has four duplicated *HK* genes, with *Hex-A* being the most conserved and essential flight muscle *HK* isozyme among *Drosophila* species [51], [52]. For *D. citri*, one of the copies of *HK* type 2-2 (Dcitr03g19430.1.1) showed moderate expression in the male and female thorax. In contrast, another copy *HK* type 2-3 (Dcitr06g14200.1.1), was highly expressed in the adult gut and midgut when compared to *HK* type 2-2 and its overall expression (Fig. 4)

*PGI* catalyzes the interconversion of glucose-6-phosphate and fructose-6-phosphate in the second step of glycolysis. Consistent with the gene copy number of *PGI* for orthologs in other insects, such as *D. melanogaster, Apis mellifera*, *Acyrthosiphon pisum*, and *Tribolium castaneum,* a single copy of *PGI* (Dcitr00g06460.1.1) was found. Expression for *PGI* is high in the male and female thorax (Fig. 4).

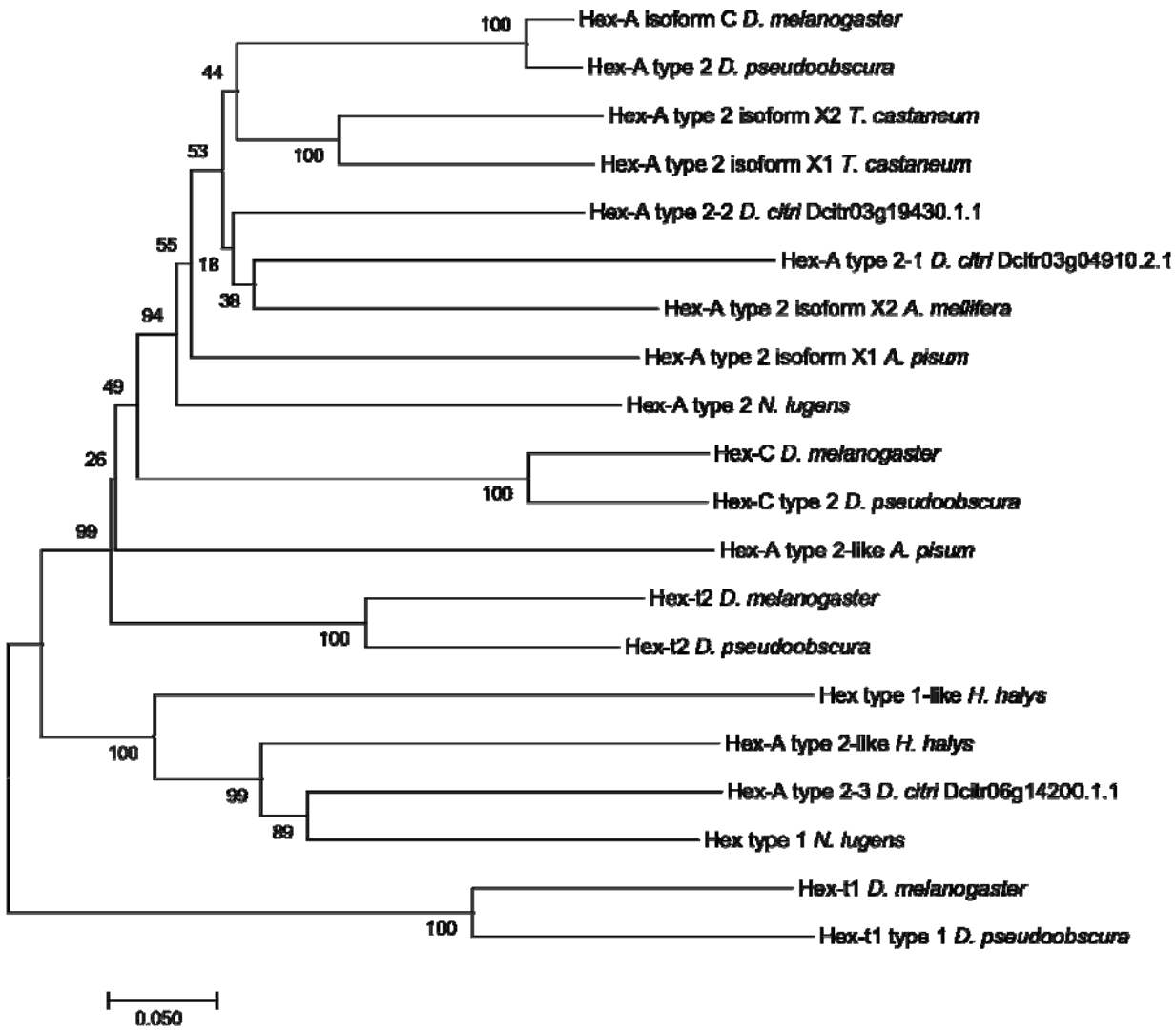


**Figure 3: Phylogenetic analysis of *hexokinase* (*HK*).** *Hexokinase* amino acid sequence of *D. citri* compared with sequences from other insects. MUSCLE multiple sequence alignments of *HK* in *D. citri* and orthologs were performed on MEGA7 and neighbor joining phylogenetic trees were constructed with p-distance for determining evolutionary distance and 1000 bootstrapping replicates [41]. The accession numbers of the orthologous sequences used in the phylogenetic analysis can be located in Table 1.

**Table 1: Accession Numbers**.

| Protein | ***Drosophila melanogaster*** | ***Tribolium castaneum*** | ***Apis mellifera*** | ***Acyrthosiphon pisum*** | ***Drosophila pseudoobscura*** | ***Halyomorpha halys*** | ***Nilaparvata lugens*** |
|---|---|---|---|---|---|---|---|
| Hex-A | NP_001259384.1 | XP_008201714.1 XP_970645.1 | XP_006557646.1 | XP_003242238.1 XP_001952412.1 | XP_001355083.1 | | XP_022204875.1 |
| Hex-type 1 | | | | | | XP_014282249.1 | XP_022184109.1 |
| Hex-type 2 | | | | | | XP_014282721.1 | |
| Hex-C | NP_524674.1 | | | | XP_001360104.2 | | |
| Hex-t1 | NP_788744.1 | | | | XP_001359146.2 | | |
| Hex-t2 | NP_733151.2 | | | | XP_002137641.2 | | |

The accession numbers for *hexokinase* orthologs were obtained from the NCBI database.

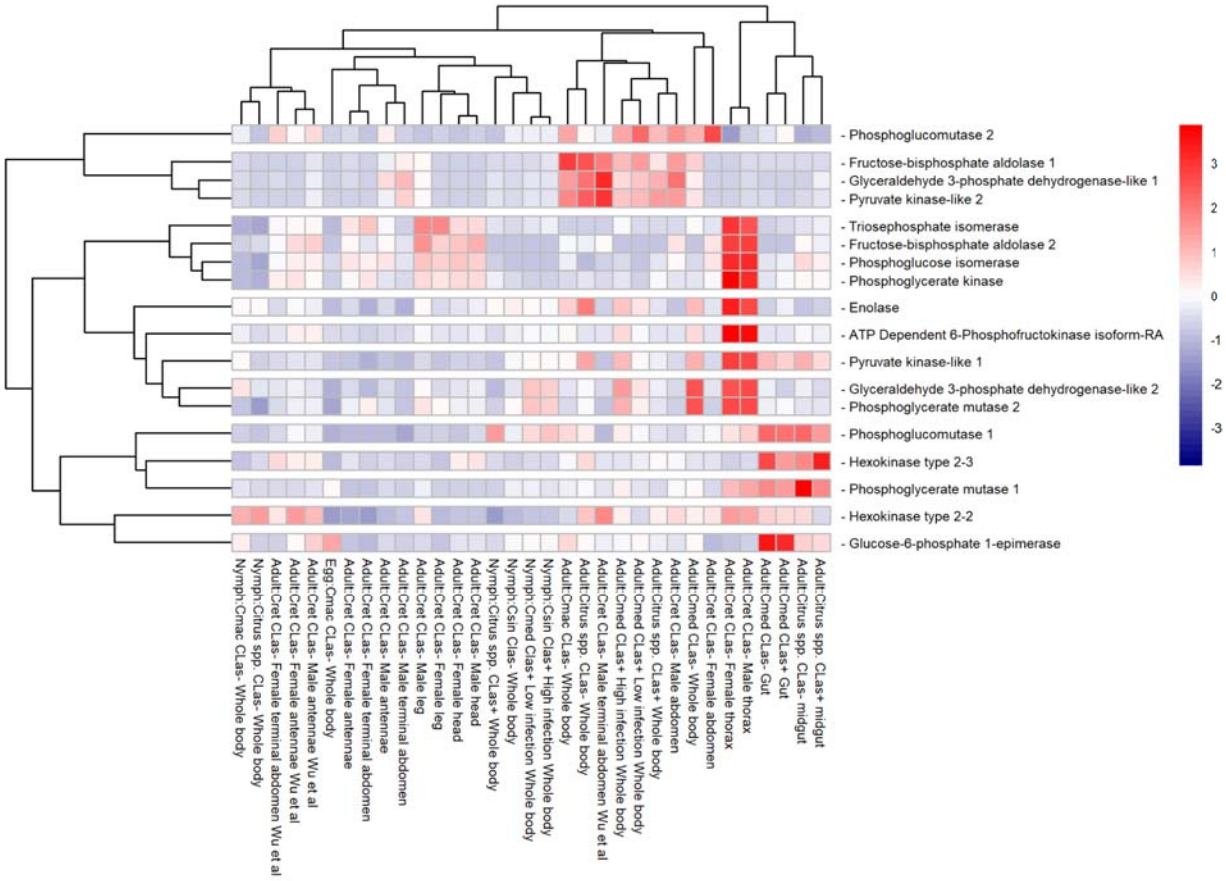


**Figure 4: Comparison of RNA-Seq datasets of genes involved in glycolysis**

The heatmap shows results from *D. citri* reared on various citrus varieties, both infected and uninfected with *C*Las. Expression values were collected from CGEN [36]. Data in the heatmap shows transcripts per million scaled by gene. RNA-seq data is available from NCBI Bioproject's PRJNA609978 and PRJNA448935 and in addition to several published data sets [9], [53] [54], [55], [56]. Expression data for *HK type 2-1* (Dcitr03g04910.2.1) is not present in the heatmap.

*PFK*, which catalyzes the phosphorylation of fructose-6-phosphate using ATP to generate fructose-1,6-bisphosphate and ADP, is the key regulatory enzyme controlling glycolysis in insects, as it catalyzes a rate-determining reaction [57], [58]. One copy of

*PFK* (Dcitr01g16570.1.1) was found and annotated in *D. citri* (Table 3). *Aldolase* catalyzes the fourth step, the reversible aldol cleavage of fructose-1,6-bisphosphate to form two trioses, glyceraldehyde-3-phosphate (GAP) and dihydroxyacetone phosphate (DHAP). Although most insects have a single copy of this gene, two well supported copies were found in *D. citri* (Table 3 and 4). One of the *aldolase* annotated copies, *fructose-bisphosphate aldolase 1*, (Dcitr04g02510.1.1) appears to have moderate expression in the male abdomen and terminal abdomen and highest expression in the adult whole body (Fig. 4). *TPI* catalyzes the fifth step, the reversible interconversion of DHAP and GAP. *TPI* is also important to sustain DHAP to maintain insect flight muscle activity [59]. *D. citri* contains a single copy of this gene (Dcitr10g08030.1.1), which is consistent with other insects (Table 3). Expression of several of these genes in the investment phase were shown to be high in the male and female thorax, especially in *PFK* (Dcitr01g16570.1.1), *fructose-bisphosphate aldolase 2* (Dcitr11g09140.1.1), and *TPI* (Dcitr10g08030.1.1) (NCBI BioProject PRJNA448935) (Fig. 4, Appendix Table 3).

**Table 3: Gene Copy Number**

| **Genes** | ***D. citri*** | ***A. pisum*** | ***T. castaneum*** | ***A. mellifera*** | ***D. melanogaster*** |
|---|---|---|---|---|---|
| *Hexokinase* (*HK*) | 3 | 3 | 2 | 1 | 4 |
| *Phosphoglucose isomerase* (*PGI*) | 1 | 1 | 1 | 1 | 1 |
| *Glucose-6-phosphate 1-epimerase* | 1 | 1 | 1 | 1 | 1 |
| *ATP Dependent 6-Phosphofructokinase* (*PFK*) | 1 | 2 | 1 | 1 | 1 |
| *Fructose bisphosphate-aldolase* (*ALDA or ALDOA*) | 2 | 1 | 1 | 1 | 1 |
| *Triosephosphate isomerase* (*TPI*) | 1 | 1 | 1 | 1 | 1 |

| | | | | | |
|---|---|---|---|---|---|
| *Glyceraldehyde-3-phosphate dehydrogenase* (*GAPDH*) | 2 | 1 | 2 | 2 | 2 |
| *Phosphoglycerate kinase* (*PGK*) | 1 | 1 | 1 | 1 | 1 |
| *Phosphoglycerate mutase* (*PGAM*) | 2 | 1 | 2 | 1 | 2 |
| *Enolase* | 1 | 1 | 3 | 2 | 1 |
| *Pyruvate kinase* (*PYK*) | 2 | 1 | 4 | 6† | 6† |
| *Pyruvate carboxylase* (*PC*) | 1 | 1 | 1 | 1 | 1 |
| *Phosphoenolpyruvate carboxykinase* (*PEPCK*) | 2 | 1 | 1 | 1 | 1 |
| *Phosphoglucomutase 1* (*PGM1*) | 1 | 1 | 1 | 1 | 1 |
| *Phosphoglucomutase 2* (*PGM2*) | 1 | 1 | 1 | 0 | 2* |
| *Aldose 1-epimerase* (*GALM*) | 2 | 3 | 2 | 3 | 1 |
| *Fructose 1,6-bisphosphatase* (*FBPase*) | 1 | 2 | 1 | 2 | 1 |
| *Glucose-6-phosphatase* (*G6P*) | 0 | 0 | 0 | 0 | 1 |
| *Trehalose-6-phosphate synthase* (*TPS*) | 2 | 1 | 2 | 1 | 1 |
| *Trehalose-6-phosphate phosphatase* (*TPP*) | 0 | 0 | 0 | 0 | 0 |
| *Trehalase 1* (*TREH-1*) | 1 | 1 | 1 | 1 | 1 |
| *Trehalase 2* (*TREH-2*) | 1 | 0 | 1 | 0 | 0 |
| *Trehalose transporter 1* (*TRET-1*) | 1 | 1 | 1 | 1 | 1 |
| *Trehalose transporter 2* (*TRET-2*) | 1 | 1 | 1 | 1 | 1 |
| *Glucose transporter* (*GLUT 1*) | 1 | 1 | 1 | 1 | 1 |

The number of genes identified in glycolysis, gluconeogenesis and trehaloneogenesis in *D. citri* and related organisms. † indicates that there are possibly more *PYK* genes in *D. melanogaster* and potentially six in *A. mellifera*. * indicates that there is *phosphoglucomutase 2a* and *2b* in *D. melanogaster*. Copy numbers for the orthologs were obtained from NCBI [39], OrthoDB [60], and Flybase [61].

**Energy production phase of Glycolysis**

*GAPDH* catalyzes the reversible conversion of GAP to 1,3-bisphosphoglycerate during glycolysis. Two *GAPDH* genes were annotated in *D. citri* and the expression data for the two paralogs show that *GAPDH-like 1* (Dcitr10g11030.1.1) has higher expression in the male terminal abdomen and whole body and *GAPDH-like 2* (Dcitr01g03200.1.1) has higher expression values overall with a considerable increase in male thorax, female thorax and whole body (NCBI BioProject PRJNA609978, NCBI BioProject PRJNA448935) (Fig. 4, Appendix Table 4). *PGK* catalyzes the reversible conversion of 1,3-bisphosphoglycerate to 3-phosphoglycerate (3PG) while generating one molecule of ATP in the seventh step of glycolysis. A single gene was annotated in *D. citri*, and other insects also have single copies (Table 3). *PGAM* is an enzyme that converts 3-phosphoglycerate to 2-phosphoglycerate. Members of the *PGAM* family share a common *PGAM* domain, and function as either phosphotransferases or phosphohydrolases [62]. Two copies of *PGAM* were annotated in the *D. citri* genome (Table 3). *PGAM 1* (Dcitr03g11640.1.1) has high expression evident in the midgut and the other paralog, *PGAM 2* (Dcitr03g17850.1.1) is highly expressed in the whole body (Fig. 4).

*Enolase* catalyzes the conversion of 2-phosphoglycerate to phosphoenolpyruvate in the ninth step of the glycolytic pathway and a single copy was annotated in the *D. citri* genome (Table 3). RNAi knockdown of the *α-enolase* in *Nilaparvata lugens* reduced egg production, offspring, and hatching rate; however, mortality of adults was unaffected [63]. Pairwise alignment between the *N. lugens* and *D. citri* sequences reveal the characteristics of the *enolase* family: a hydrophobic domain (AAVPSGASTGI) in the N-

terminal region at position 31-41, a seven amino acid substrate binding pocket (H159, E211, K345, HRS373-375, and K396), a metal-binding site (S38, D246, E295, and D320) and the *enolase* signature motif (LLLKVNQIGSVTES) [63].

*PYK* catalyzes the irreversible transfer of a phosphoryl group from phosphoenolpyruvate to ADP; thus generating pyruvate and a second ATP molecule, the end products of the glycolysis reaction. The copy number of *PYK* varies among insects; *A. mellifera* and *D. melanogaster* both contain six, and *A. gambiae* has only one (Table 3). In *D. citri,* two *PYK* genes were characterized and annotated (Appendix Table 2). One of the *PYK* genes (Dcitr07g06140.1.1) is highly expressed in male and female thorax and the other *PYK* gene (Dcitr01g11190.1.1) has relatively low overall expression with the highest expression in the male terminal abdomen (Fig. 4). Expression analysis of the enzymes from this phase of glycolysis in thoracic tissue shows that the highest expression is observed for *GAPDH-like 2* and *PYK-like 1* and the lowest occurs for both *GAPDH-like 1* and *PYK-like 2* (Fig. 5). In addition, *PGK* (Dcitr00g01740.1.1) and *enolase* (Dcitr02g07600.1.1) also have high expression in the male and female thorax and *PGAM2* (Dcitr03g17850.1.1) has high expression in whole body besides the male and female thorax (NCBI BioProject PRJNA609978, NCBI BioProject PRJNA448935) (Fig. 4, Appendix Table 4).

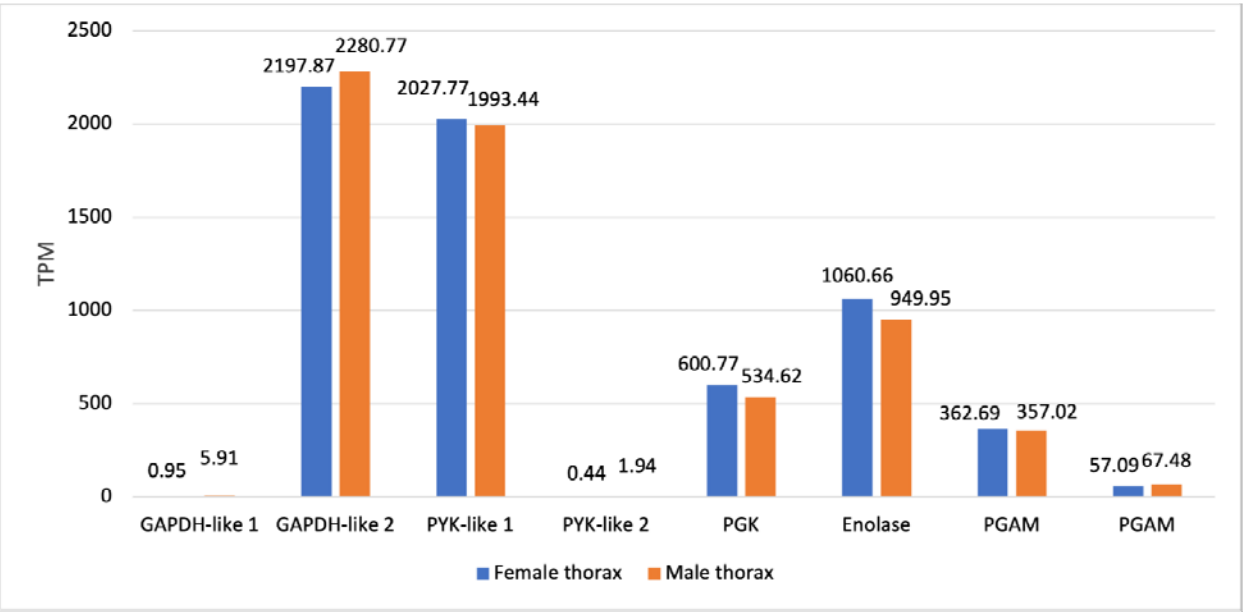


**Figure 5: PEN expression data for the enzymes involved during the energy production phase in *D. citri.*** (*GAPDH-like 1*: Dcitr10g11030.1.1; *GAPDH-like 2*: Dcitr01g03200.1.1; *PYK-like 1*: Dcitr07g06140.1.1; *PYK-like 2*: Dcitr01g11190.1.1; *PGK*: Dcitr00g01740.1.1; *Enolase*: Dcitr02g07600.1.1; *PGAM*: Dcitr03g17850.1.1, Dcitr03g11640.1.1 respectively). Values are based on transcripts taken from the thorax of healthy *C*Las- *D. citri* male and female adults that fed on *C. reticulata*. These experiments had a single replicate. RNA-seq data is available from NCBI BioProject's PRJNA448935.

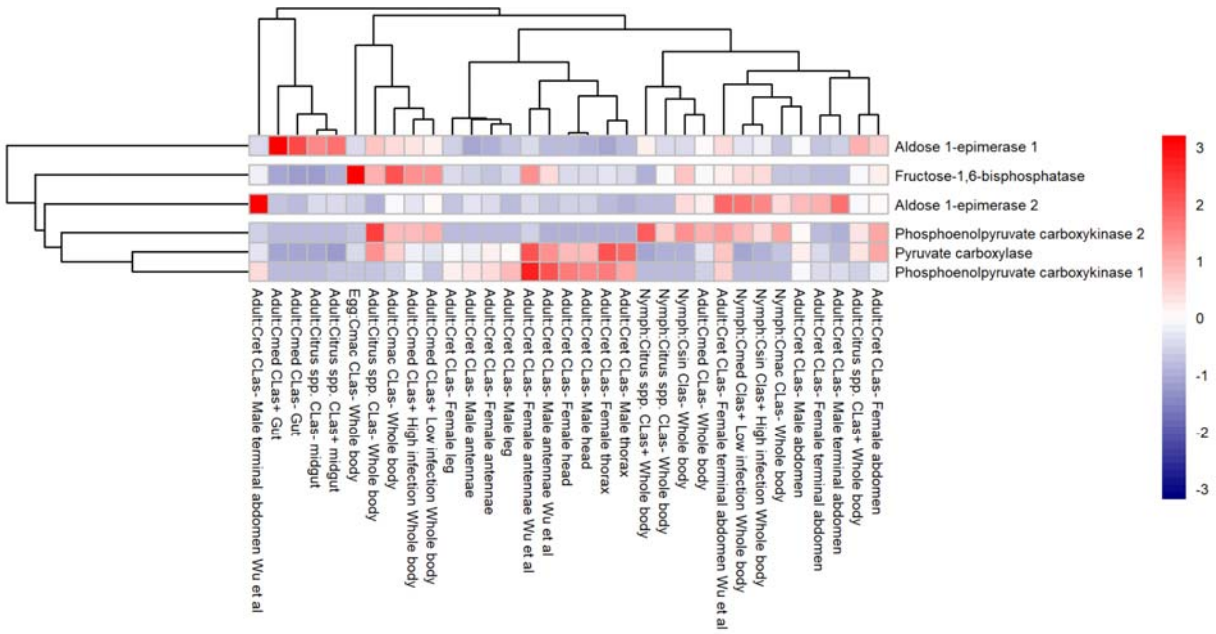


**Figure 6: Comparison of RNA-Seq datasets of genes involved in gluconeogenesis**

The heatmap shows results from *D. citri* reared on various citrus varieties, both infected and uninfected with *C*Las. Expression values were collected from Citrus Greening expression network [36]. Data in the heatmap shows transcripts per million scaled by gene. RNA-seq data is available from NCBI Bioprojects PRJNA609978 and PRJNA448935 and published data sets [53].

**Enzymes of Gluconeogenesis**

Gluconeogenesis is the metabolic process to re-generate glucose from non-carbohydrate substrates and uses four specific enzymes. *PC* catalyzes the ATP-dependent carboxylation of pyruvate to oxaloacetate. The curated *PC* model (Dcitr08g01610.1.1) in *D. citri* shows highest overall expression in the male and female thorax, male and female head, and male and female antenna (Fig. 6, Fig. 7, Appendix Table 5). *PEPCK* controls the cataplerotic flux and converts oxaloacetate from the

tricarboxylic acid cycle to form PEP. Two *PEPCK* genes were annotated and characterized in the *D. citri* genome (Appendix Table 2). The first *PEPCK* copy (Dcitr05g10240.1.1) has the highest expression in most tissues compared to all of the gluconeogenesis genes as is evident in the male and female antenna, male and female thorax, and the male and female head. The highest expression of the second copy of *PEPCK* (Dcitr08g02760.1.1) is shown in the whole body. *FBPase* facilitates one of the three bypass reactions occurring in gluconeogenesis where the hydrolysis of fructose-1,6-bisphosphate produces fructose-6-phosphate. A single copy of this gene was annotated in *D. citri,* which is comparable to other insects, although two copies are present in the pea aphid, *A. pisum,* and honey bee, *A. mellifera* (Table 3). *FBPase* (Dcitr11g08070.1.1) shows highest expression in the egg (Fig. 5). *Glucose-6-phosphatase* (*G6Pase* or *G6P*), which is specific to gluconeogenesis, catalyzes the conversion of glucose-6-phosphate to glucose [27]. However, this enzyme is not present in most insect species, including *D. citri.* Though present in *N. lugens*, RNAi studies showed that knockdown of *G6Pase* in *N. lugens* had no effect on the genes involved in trehalose metabolism [64].

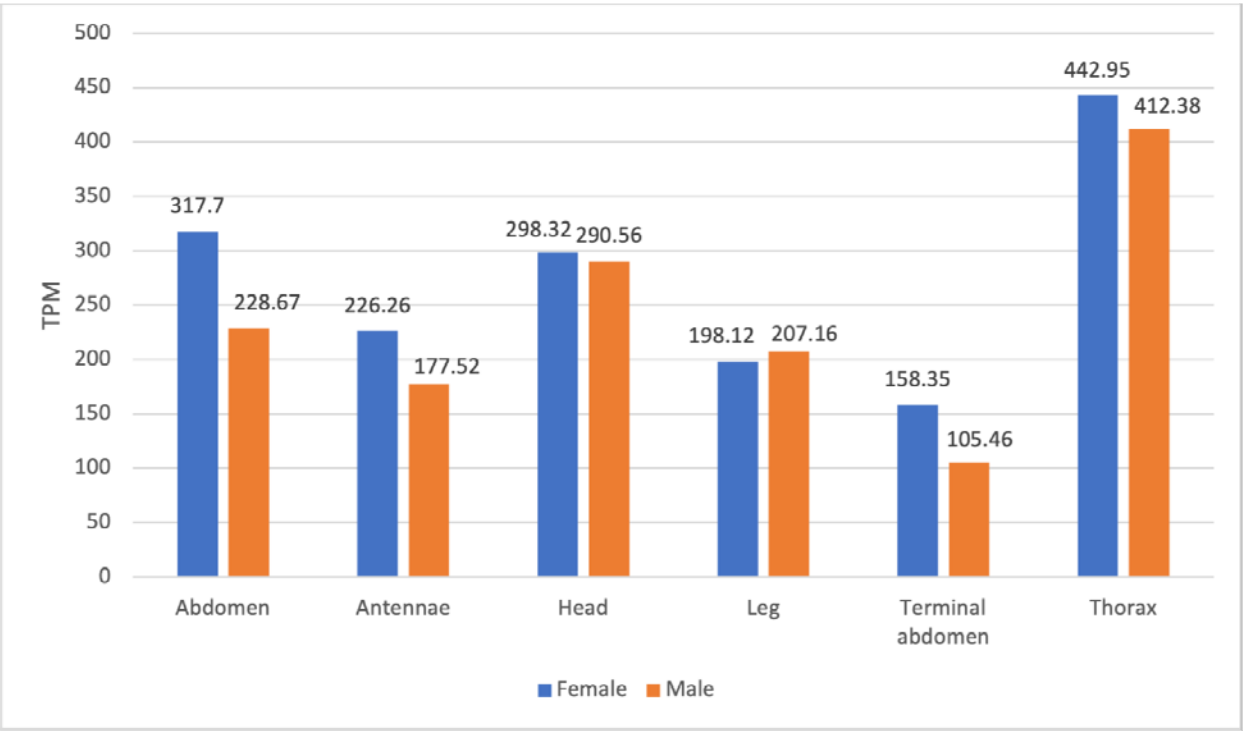


**Figure 7: PEN Expression data of the enzyme *Pyruvate carboxylase* (Dcitr08g01610.1.1) in *D. citri*.** Values are based on transcripts isolated from various body parts of healthy *C*Las- *D. citri* adults that fed on *C. reticulata.* These experiments had a single replicate. RNA-seq data is available from NCBI BioProjects PRJNA448935.

**Enzymes of Trehaloneogenesis**

Trehalose is a nonreducing disaccharide that is present in many organisms, including yeast, fungi, bacteria, plants and invertebrates and is in high concentration as the main hemolymph sugar in insects [28], [65]. Trehalose is synthesized from glucose by trehalose-6-phosphate (Tre-6-P), where the mobilization of trehalose to glucose is considered critical for metabolic homeostasis in insect physiology [26]. Synthesis of trehalose occurs in the fat body, when stimulated by neuropeptides from the brain [28]. These peptides decrease the concentration of fructose 2,6-bisphosphate which strongly

activates the glycolytic enzyme *PFK* and inhibits the gluconeogenic enzyme *fructose 1,6-bisphosphatase*. *Fructose 2,6-bisphosphatase* is thus a key metabolic signal in regulating trehalose synthesis in insects. After synthesis, trehalose is transported through the hemolymph and enters cells through *trehalose transporters*, where it is converted into glucose by trehalase.

There are three enzymes involved in trehaloneogenesis: *trehalose-6-phosphate synthase* (*TPS*), *trehalose-6-phosphate phosphatase* (*TPP*), and *trehalase* (*TREH*) (Fig. 1). *TPS* catalyzes the transfer of glucose from UDP-glucose to G6P forming trehalose 6-phosphate (T6P) and UDP [66]. A *TPS* (*DcTPS*) gene has been targeted in *D. citri* for RNAi therapeutics and the results suggested that dsRNA-mediated gene specific silencing resulted in a strong reduction in expression of *DcTPS* and survival rate of nymphs and an increase in malformation [67]. Two copies of *TPS* were annotated in the v3 genome of *D. citri*. *TPS 1* (Dcitr02g17550.1.1) had the highest expression found in the *C*Las+ and *C*Las- adult midgut, respectively (Fig. 9, Appendix Table 6). In some organisms, *TPP* dephosphorylates T6P to trehalose and inorganic phosphate [66]. However, many insects appear to lack this gene, including *D. citri* as it was not found in the v3 genome. Most insects with multiple *TPS* genes encode proteins with TPS and TPP domains [68], [69]. *TPS* in *Drosophila* appears to have the functions of both *TPS* and *TPP* [70]. *Trehalase* (*TREH*) catalyzes stored trehalose by cleaving it to two glucose molecules. There are two trehalase genes: *TREH-1*, which encodes a soluble enzyme found in haemolymph, goblet cell cavity and egg homogenates, and *TREH-2*, which encodes a membrane-bound enzyme found in flight muscle, ovary,

spermatophore, midgut, brain and thoracic ganglia [66]. The two curated *TREH* genes in *D. citri* show different expression in the psyllid. *TREH-1A* (Dcitr07g04030.1.1) shows high expression in the gut and midgut and *TREH*-2 (Dcitr08g09220.1.1) shows moderate expression in the female thorax and male antennae (Fig. 8). *TREH* is the only enzyme known for the irreversible splitting of trehalose in all insects [66] and *D. citri and T. castaneum* are the only insects with the second copy, *TREH-2* (Table 3).

The two main *trehalose transporters* are *trehalose transporter 1* (*TRET1*) and *trehalose transporter 2* (*TRET2*), which both transport trehalose to and from cells with *TREH*. One gene copy for each of these *trehalose transporters* was annotated in *D. citri* (Appendix Table 2) and expression analysis shows that *TRET1* (Dcitr01g17710.1.1) is highly expressed in the gut and *TRET2* (Dcitr00g03240.1.1) is moderately expressed in the male abdomen (Fig. 8).

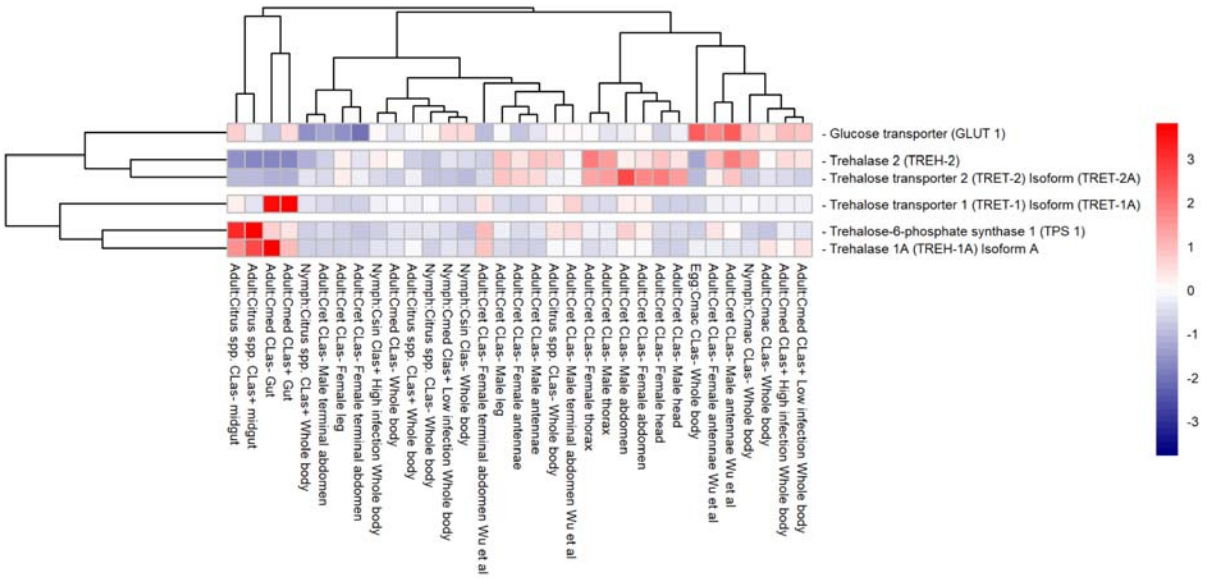

**Figure 8: Comparison of RNA-Seq datasets of genes involved in trehaloneogenesis**

The heatmap shows results from *D. citri* reared on various citrus varieties, both infected and uninfected with *C*Las. Expression values were collected from Citrus Greening expression network [36]. Data in the heatmap shows transcripts per million scaled by gene. RNA-seq data is available from NCBI Bioproject's PRJNA609978 and PRJNA448935 and published data sets [53]. Expression data for *Trehalose-6-phosphate synthase 2* (*TPS 2*), *Trehalase 2* (*TREH-2*), *Trehalose transporter 1* (*TRET-1*) *Isoform* (*TRET-1B*), *Trehalose transporter 2* (*TRET-2*) *Isoform* (*TRET-2B*), and *Trehalose transporter 2* (*TRET-2*) *Isoform* (*TRET-2C*) are not present in the heatmap.

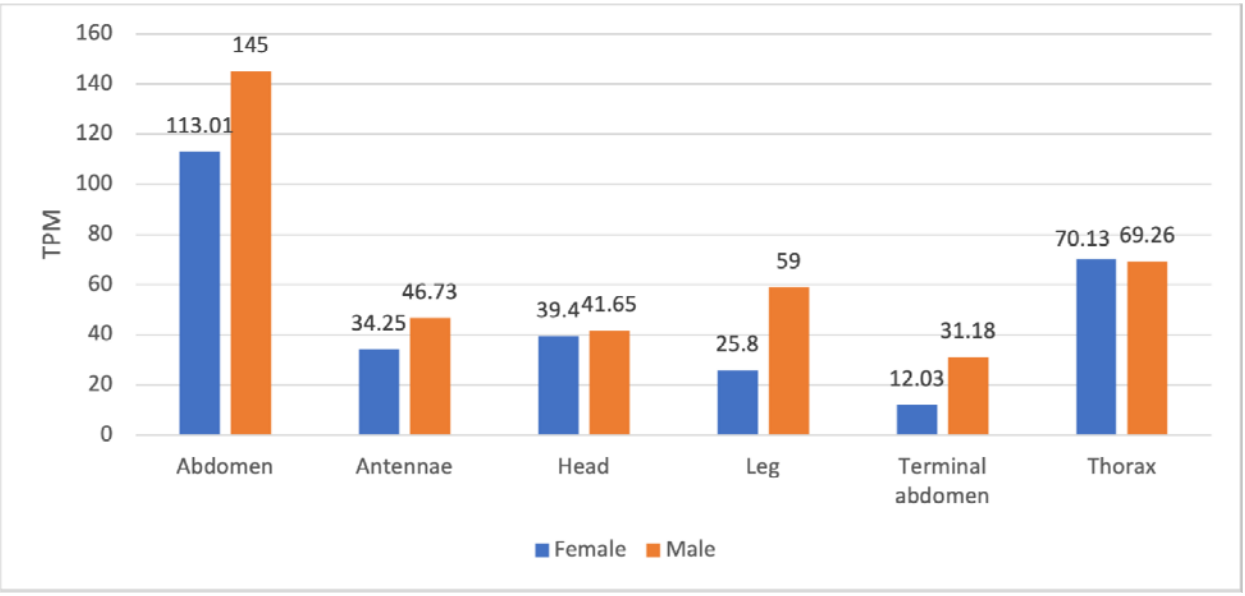


**Figure 9: PEN Expression data of the enzyme *Trehalose 6-phosphate synthase* (Dcitr02g17550.1.1) in *D. citri*.** Values are based on transcripts expressed in various body parts of healthy *C*Las- *D. citri* adults that fed on *C. reticulata*. These experiments

had a single replicate. RNA-seq data is available from NCBI BioProject PRJNA448935.

## Conclusion

Manual curation of genes in the glycolysis, gluconeogenesis, and trehaloneogenesis pathways was completed in the genome of *D. citri*. Twenty-five genes were annotated in glycolysis and gluconeogenesis. The pathways are highly conserved and copy numbers of the genes annotated were comparable to other insects. Except for *G6Pase*, all enzymes involved in glycolysis and gluconeogenesis were identified. An additional seven genes involved in trehaloneogenesis were also identified and annotated. Manual annotation of these central metabolic pathways provides accurate gene models which are required for development of molecular therapeutics to target *D. citri*. RNAi studies targeting genes involved in trehalose metabolism produced significant mortality in *D. citri*, [67], [71] demonstrating the functional application of the genes identified. Expression analysis of the genes annotated in the carbohydrate metabolism pathways identified differences related to life stage, sex and tissue. This data advances the understanding of the basic biology of *D. citri* and will aid in the development of RNAi-based applications.

## Reuse potential

The manually curated gene models were annotated through a collaborative community project [11] to further understand psyllid biology and with a goal to annotate gene families related to immune response, metabolism and other major functions [72]. Continued examination of the glycolysis, gluconeogenesis, and trehaloneogenesis

pathways across arthropods, and especially in insect vectors like *D. citri*, will provide novel and species-specific gene targets to control psyllid populations (potentially through the use of RNAi) and reduce the effects of pathogens such as *C*Las.

**Data availability**

The datasets supporting this article are available in the *GigaScience* GigaDB repository [REF].

The gene models will be part of an updated official gene set (OGS) for *D. citri* that will be submitted to NCBI. The OGS (v3) will also be publicly available for download, BLAST analysis and expression profiling on Citrusgreening.org and the Citrus Greening Expression Network [36]. The *D. citri* genome assembly (v3), OGS (v3) and transcriptomes are accessible on the Citrusgreening.org portal [73]. Accession numbers for genes used in multiple alignments or phylogenetic trees are provided in Table 1.

**Declarations**

**List of Abbreviations**

ADP: adenosine diphosphate; *Am*: *Apis mellifera*; *Ap*: *Acyrthosiphon pisum*; ATP: adenosine triphosphate; BLASTp: protein BLAST; CGEN: Citrus Greening Expression Network; *C*Las: *Candidatus* Liberibacter asiaticus; *Cmac*: *C. macrophylla; Cmed*: *C. medica*; *Cret*: *C. reticulata*; *Csin*: *C. sinensis*; *Dc*: *Diaphorina citri*; DHAP: dihydroxyacetone phosphate; *Dm*: *Drosophila melanogaster*; *FBPase*: *fructose-1,6-*

*bisphosphatase*; GAP: glyceraldehyde-3-phosphate; *GAPDH*: *glyceraldehyde 3-phosphate dehydrogenase*; *G6Pase/G6P*: *glucose-6-phosphatase*; *Hh*: *Halyomorpha halys*; *HK*: *hexokinase*; Iso-seq: Isoform sequencing; MCOT: Maker, Cufflinks, Oasis, Trinity; NADH: nicotinamide adenine dinucleotide (reduced form); NAD+: nicotinamide adenine dinucleotide (oxidized form); NCBI: National Center for Biotechnology Information; *Nl*: *Nilaparvata lugens*; *PC*: *pyruvate carboxylase*; *PEPCK*: *phosphoenolpyruvate carboxykinase*; *PFK*: *phosphofructokinase*; *PGAM*: *phosphoglycerate mutase*; *PGI*: *phosphoglucose isomerase*; *PGK*: *phosphoglycerate kinase*; *PYK*: *pyruvate kinase*; RNAi: RNA interference; RNA-seq: RNA sequencing; *Tc*: *Tribolium castaneum*; *TPI*: *triosephosphate isomerase*; TPM: transcripts per million; *TPP*: *trehalose-6-phosphate phosphatase*; *TPS*: *trehalose-6-phosphate synthase*; TRE: trehalose; TZP: triazophos; T6P: trehalose-6-phosphate.

**Ethical Approval**

Not applicable.

**Consent for publication**

Not applicable.

**Competing Interests**

The authors declare that they have no competing interests.

## Authors' Contributions

WBH, SJB, TD and LAM conceptualized the study; TD, SS, TDS and SJB supervised the study; SJB, TD, SS and LAM contributed to project administration; BT, AM, KK, CV, CM, DH and SA conducted investigation; PH, MF-G, NP and SS contributed to software development; PH, MF-G, SS, TDS and JB developed methodology; SJB, TD, WBH and LAM acquired funding; BT, DLH, MRJ, AM and KK prepared and wrote the original draft; TD, SJB, SS, NP, TDS, WBH and JB reviewed and edited the draft.

## Funding

This work was supported by USDA-NIFA grants 2015-70016-23028, HSI 2020-38422-32252 and 2020-70029-33199.

USDA, NIFA, National Institute of Food and Agriculture, Citrus Greening award #2015-70016-23028," Developing an Infrastructure and Product Test Pipeline to Deliver Novel Therapies for Citrus Greening Disease";

## Acknowledgements

We would like to thank Helen Wiersma-Koch (Indian River State College) and Thomson Paris (USDA-ARS-Horticultural Research Laboratories) for assistance.

## References


1. Bové JM. HUANGLONGBING: A DESTRUCTIVE, NEWLY-EMERGING, CENTURY-OLD DISEASE OF CITRUS. *J Plant Pathol*. Società Italiana di Patologia Vegetale (SIPaV); 88:7–372006;

2. Haapalainen M. Biology and epidemics of CandidatusLiberibacter species, psyllid-transmitted plant-pathogenic bacteria. *Ann Appl Biol*. Wiley; 165:172–982014;

3. Wang N, Pierson EA, Setubal JC, Xu J, Levy JG, Zhang Y, et al.. The Candidatus Liberibacter–Host Interface: Insights into Pathogenesis Mechanisms and Disease Control. *Annu Rev Phytopathol*. Annual Reviews; 55:451–822017;

4. Wang N, Stelinski LL, Pelz-Stelinski KS, Graham JH, Zhang Y. Tale of the Huanglongbing Disease Pyramid in the Context of the Citrus Microbiome. *Phytopathology*. 107:380–72017;

5. Halbert SE, Manjunath KL. ASIAN CITRUS PSYLLIDS (STERNORRHYNCHA: PSYLLIDAE) AND GREENING DISEASE OF CITRUS: A LITERATURE REVIEW AND ASSESSMENT OF RISK IN FLORIDA. *flen*. Florida Entomological Society; 87:330–532004;

6. Hall DG, Richardson ML, Ammar E-D, Halbert SE. Asian citrus psyllid,Diaphorina citri, vector of citrus huanglongbing disease. Entomologia Experimentalis et Applicata.

7. Yamamoto PT, Fellipe MR, Sanches AL, Coelho JHC, Garbim LF, Ximenes NL. Eficácia de Inseticidas para o Manejo de Diaphorina citri Kuwayama (Hemiptera: Psyllidae) em Citros. BioAssay.

8. Tiwari S, Mann RS, Rogers ME, Stelinski LL. Insecticide resistance in field populations of Asian citrus psyllid in Florida. Pest Management Science.

9. Reese J, Christenson MK, Leng N, Saha S, Cantarel B, Lindeberg M, et al.. Characterization of the Asian Citrus Psyllid Transcriptome. *J Genomics*. 2:54–82014;

10. Saha S, Hosmani PS, Flores-Gonzalez M, Hunter W, D'Elia T. Biocuration and improvement of the Diaphorina citri draft genome assembly with long reads, optical maps and long-range scaffolding. *International Psyllid Annotation Consortium, Proceedings of 10th Arthropod Genomics Symposium, June 8*. p. 27–8.

11. Saha S, Hosmani PS, Villalobos-Ayala K, Miller S, Shippy T, Flores M, et al.. Improved annotation of the insect vector of citrus greening disease: biocuration by a diverse genomics community. *Database* . 2019; doi: 10.1093/database/baz035.

12. Andrade EC, Hunter WB. RNAi feeding bioassay: development of a non-transgenic approach to control Asian citrus psyllid and other hemipterans. *Entomol Exp Appl*. Wiley; 162:389–962017;

13. Ghosh SKB, Hunter WB, Park AL, Gundersen-Rindal DE. Double strand RNA delivery system for plant-sap-feeding insects. PLOS ONE.

14. Ghosh SKB, Hunter WB, Park AL, Gundersen-Rindal DE. Double-stranded RNA Oral Delivery Methods to Induce RNA Interference in Phloem and Plant-sap-feeding Hemipteran Insects. *J Vis Exp*. 2018; doi: 10.3791/57390.

15. Hunter WB, Sinisterra-Hunter XH. Chapter Six - Emerging RNA Suppression Technologies to Protect Citrus Trees From Citrus Greening Disease Bacteria. In: Smagghe G, editor. *Advances in Insect Physiology*. Academic Press; p. 163–97.

16. Killiny N, Kishk A. Delivery of dsRNA through topical feeding for RNA interference in the citrus sap piercing-sucking hemipteran, Diaphorina citri. *Arch Insect Biochem Physiol*. Wiley; 95:e213942017;

17. Kishk A, Anber HAI, AbdEl-Raof TK, El-Sherbeni A-HD, Hamed S, Gowda S, et al.. RNA interference of carboxyesterases causes nymph mortality in the Asian citrus psyllid, Diaphorina citri. *Arch Insect Biochem Physiol*. 2017; doi: 10.1002/arch.21377.

18. Yu X, Killiny N. RNA interference of two glutathione S-transferase genes, Diaphorina citri DcGSTe2 and DcGSTd1 , increases the susceptibility of Asian citrus psyllid (Hemiptera: Liviidae) to the pesticides fenpropathrin and thiamethoxam. Pest Management Science.

19. Hunter WB, Clarke S-KV, Mojica AFS, Paris TM, Miles G, Metz JL, et al.. Advances in RNA suppression of the Asian citrus psyllid vector and bacteria (huanglongbing pathosystem). *Asian Citrus Psyllid: Biology, Ecology and Management of the Huanglongbing Vector Wallingford: CABI*. :258–842020;

20. Yu H-Z, Huang Y-L, Lu Z-J, Zhang Q, Su H-N, Du Y-M, et al.. Inhibition of trehalase affects the trehalose and chitin metabolism pathways in Diaphorina citri (Hemiptera: Psyllidae). *Insect Sci*. 28:718–342021;

21. Sandoval-Mojica AF, Altman S, Hunter WB, Pelz-Stelinski KS. Peptide conjugated morpholinos for management of the huanglongbing pathosystem. *Pest Manag Sci*. Wiley; 76:3217–242020;

22. Hunter WB, Gonzalez MT, Tomich J. BAPC-assistedCRISPR/Cas9 System: Targeted Delivery into Adult Ovaries for Heritable Germline Gene Editing (Arthropoda: Hemiptera).

23. Hunter WB, Gonzalez MT, Tomich J. BAPC-assisted -CRISPR-Cas9 delivery into nymphs and adults for heritable gene editing (Hemiptera). *FASEB J*. Wiley; 2019; doi: 10.1096/fasebj.2019.33.1_supplement.626.2.

24. Bretscher H, O'Connor MB. The Role of Muscle in Insect Energy Homeostasis. *Front Physiol*. 11:5806872020;

25. Crabtree B, Newsholme EA. The activities of phosphorylase, hexokinase, phosphofructokinase, lactate dehydrogenase and the glycerol 3-phosphate dehydrogenases in

muscles from vertebrates and invertebrates. *Biochem J*. 126:49–581972;

26. Matsuda H, Yamada T, Yoshida M, Nishimura T. Flies without trehalose. *J Biol Chem*. 290:1244–552015;

27. Miyamoto T, Amrein H. Gluconeogenesis: An ancient biochemical pathway with a new twist. *Fly* . 11:218–232017;

28. Becker A, Schlöder P, Steele JE, Wegener G. The regulation of trehalose metabolism in insects. *Experientia*. 52:433–91996;

29. Tournu H, Fiori A, Van Dijck P. Relevance of trehalose in pathogenicity: some general rules, yet many exceptions. *PLoS Pathog*. 9:e10034472013;

30. Hunter WB, Gonzalez MT, Andrade EC. Double stranded RNA compositions for reducing asian citrus psyllid infestation and methods of use. US Patent.

31. Bachman P, Fischer J, Song Z, Urbanczyk-Wochniak E, Watson G. Environmental Fate and Dissipation of Applied dsRNA in Soil, Aquatic Systems, and Plants. *Front Plant Sci*. 11:212020;

32. Christiaens O, Whyard S, Vélez AM, Smagghe G. Double-Stranded RNA Technology to Control Insect Pests: Current Status and Challenges. *Front Plant Sci*. 11:4512020;

33. Fletcher SJ, Reeves PT, Hoang BT, Mitter N. A Perspective on RNAi-Based Biopesticides. *Front Plant Sci*. 11:512020;

34. Kunte N, McGraw E, Bell S, Held D, Avila L-A. Prospects, challenges and current status of RNAi through insect feeding. *Pest Manag Sci*. 76:26–412020;

35. Raybould A, Burns A. Problem Formulation for Off-Target Effects of Externally Applied Double-Stranded RNA-Based Products for Pest Control. *Front Plant Sci*. 11:4242020;

36. Flores-Gonzalez M, Hosmani PS, Fernandez-Pozo N, Mann M, Humann JL, Main D, et al.. Citrusgreening.org: An open access and integrated systems biology portal for the Huanglongbing (HLB) disease complex. bioRxiv.

37. Voet D, Pratt CW, Voet JG. Principles of Biochemistry. Wiley;

38. Hosmani PS, Shippy T, Miller S, Benoit JB, Munoz-Torres M, Flores-Gonzalez M, et al.. A quick guide for student-driven community genome annotation. *PLoS Comput Biol*. 15:e10066822019;

39. : Home - Protein - NCBI. https://www.ncbi.nlm.nih.gov/protein Accessed 2021 Sep 24.

40. Shippy TD, Others. Annotating genes in Diaphorina citri genome version 3. protocols. io. 2020.

41. Kumar S, Stecher G, Tamura K. MEGA7: Molecular Evolutionary Genetics Analysis Version 7.0 for Bigger Datasets. Molecular Biology and Evolution.

42. Hosmani PS, Flores-Gonzalez M, Shippy T, Vosburg C, Massimino C, Tank W, et al.. Chromosomal length reference assembly for Diaphorina citri using single-molecule sequencing and Hi-C proximity ligation with manually curated genes in developmental, structural and

immune pathways. bioRxiv.

43. Thurmond J, Goodman JL, Strelets VB, Attrill H, Gramates LS, Marygold SJ, et al.. FlyBase 2.0: the next generation. *Nucleic Acids Res*. 47:D759–652019;

44. Tribolium Genome Sequencing Consortium, Richards S, Gibbs RA, Weinstock GM, Brown SJ, Denell R, et al.. The genome of the model beetle and pest Tribolium castaneum. *Nature*. 452:949–552008;

45. Elsik CG, Worley KC, Bennett AK, Beye M, Camara F, Childers CP, et al.. Finding the missing honey bee genes: lessons learned from a genome upgrade. *BMC Genomics*. 15:862014;

46. International Aphid Genomics Consortium. Genome sequence of the pea aphid Acyrthosiphon pisum. *PLoS Biol*. 8:e10003132010;

47. Xue J, Zhou X, Zhang C-X, Yu L-L, Fan H-W, Wang Z, et al.. Genomes of the rice pest brown planthopper and its endosymbionts reveal complex complementary contributions for host adaptation. *Genome Biol*. 15:5212014;

48. Ma W, Xu L, Hua H, Chen M, Guo M, He K, et al.. Chromosomal-level genomes of three rice planthoppers provide new insights into sex chromosome evolution. *Mol Ecol Resour*. Wiley; 21:226–372021;

49. Sparks ME, Bansal R, Benoit JB, Blackburn MB, Chao H, Chen M, et al.. Brown marmorated stink bug, Halyomorpha halys (Stål), genome: putative underpinnings of polyphagy, insecticide resistance potential and biology of a top worldwide pest. *BMC Genomics*. 21:2272020;

50. Nation Sr JL. Insect physiology and biochemistry. content.taylorfrancis.com; 2015;

51. Adams MD. The Genome Sequence of Drosophila melanogaster. Science.

52. Duvernell DD, Eanes WF. Contrasting molecular population genetics of four hexokinases in Drosophila melanogaster, D. simulans and D. yakuba. *Genetics*. 156:1191–2012000;

53. Wu Z, Zhang H, Bin S, Chen L, Han Q, Lin J. Antennal and Abdominal Transcriptomes Reveal Chemosensory Genes in the Asian Citrus Psyllid, Diaphorina citri. *PLoS One*. 11:e01593722016;

54. Kruse A, Fattah-Hosseini S, Saha S, Johnson R, Warwick E, Sturgeon K, et al.. Combining ’omics and microscopy to visualize interactions between the Asian citrus psyllid vector and the Huanglongbing pathogen Candidatus Liberibacter asiaticus in the insect gut. PLOS ONE.

55. Vyas M, Fisher TW, He R, Nelson W, Yin G, Cicero JM, et al.. Asian Citrus Psyllid Expression Profiles Suggest Candidatus Liberibacter Asiaticus-Mediated Alteration of Adult Nutrition and Metabolism, and of Nymphal Development and Immunity. PLOS ONE.

56. Yu H-Z, Li N-Y, Zeng X-D, Song J-C, Yu X-D, Su H-N, et al.. Transcriptome Analyses of Diaphorina citri Midgut Responses to Candidatus Liberibacter Asiaticus Infection. *Insects*. 2020; doi: 10.3390/insects11030171.

57. Mordue W, Goldsworthy GJ, Brady J, Blaney WM, Others. Insect physiology. Blackwell

Scientific Publications.;

58. Currie PD, Sullivan DT. Structure and expression of the gene encoding phosphofructokinase (PFK) in Drosophila melanogaster. *J Biol Chem*. 269:24679–871994;

59. O'Brien SJ, MacIntyre RJ. Genetics and biochemistry of enzymes and specific proteins of Drosophila. *Genetics and biology of Drosophila*. 2a1978;

60. Kriventseva EV, Kuznetsov D, Tegenfeldt F, Manni M, Dias R, Simão FA, et al.. OrthoDB v10: sampling the diversity of animal, plant, fungal, protist, bacterial and viral genomes for evolutionary and functional annotations of orthologs. *Nucleic Acids Res*. 47:D807–112019;

61. Larkin A, Marygold SJ, Antonazzo G, Attrill H, Dos Santos G, Garapati PV, et al.. FlyBase: updates to the Drosophila melanogaster knowledge base. *Nucleic Acids Res*. 49:D899–9072021;

62. Takeda K, Komuro Y, Hayakawa T, Oguchi H, Ishida Y, Murakami S, et al.. Mitochondrial phosphoglycerate mutase 5 uses alternate catalytic activity as a protein serine/threonine phosphatase to activate ASK1. *Proc Natl Acad Sci U S A*. 106:12301–52009;

63. Wang W-X, -X. Wang W, -L. Li K, Chen Y, -X. Lai F, Fu Q. Identification and Function Analysis of enolase Gene NlEno1 from Nilaparvata lugens (Stal) (Hemiptera:Delphacidae). Journal of Insect Science.

64. Pan B-Y, Li G-Y, Wu Y, Zhou Z-S, Zhou M, Li C. Glucose Utilization in the Regulation of Chitin Synthesis in Brown Planthopper. *J Insect Sci*. 2019; doi: 10.1093/jisesa/iez081.

65. Elbein AD, Pan YT, Pastuszak I, Carroll D. New insights on trehalose: a multifunctional molecule. *Glycobiology*. 13:17R – 27R2003;

66. Shukla E, Thorat LJ, Nath BB, Gaikwad SM. Insect trehalase: physiological significance and potential applications. *Glycobiology*. 25:357–672015;

67. Liu X, Zou Z, Zhang C, Liu X, Wang J, Xin T, et al.. Knockdown of the Trehalose-6-Phosphate Synthase Gene Using RNA Interference Inhibits Synthesis of Trehalose and Increases Lethality Rate in Asian Citrus Psyllid, Diaphorina citri (Hemiptera: Psyllidae). *Insects*. 2020; doi: 10.3390/insects11090605.

68. Tang B, Wang S, Wang S-G, Wang H-J, Zhang J-Y, Cui S-Y. Invertebrate Trehalose-6-Phosphate Synthase Gene: Genetic Architecture, Biochemistry, Physiological Function, and Potential Applications. *Front Physiol*. 9:302018;

69. Tang B, Xu Q, Zhao L, Wang S, Zhang F, Others. Progress in research on the characteristics and functions of trehalose and the TPS gene in insects. *Chinese Journal of Applied Entomology*. Institute of Zoology; 51:1397–4052014;

70. Yoshida M, Matsuda H, Kubo H, Nishimura T. Molecular characterization of Tps1 and Treh genes in Drosophila and their role in body water homeostasis. *Sci Rep*. 6:305822016;

71. Hunter WB, Wintermantel WM. Optimizing Efficient RNAi-Mediated Control of Hemipteran Pests (Psyllids, Leafhoppers, Whitefly): Modified Pyrimidines in dsRNA Triggers. *Plants*. Multidisciplinary Digital Publishing Institute; 10:17822021;

72. : CitrusGreening.org. https://citrusgreening.org/annotation/index Accessed 2021 Sep 24.

73. : CitrusGreening.org. https://citrusgreening.org/ Accessed 2021 Sep 24.

74. Miller S, Tamayo B, Shippy TD, Hosmani PS, Flores-Gonzalez M, Mueller LA, et al.. Chitin Biosynthesis Genes in Diaphorina citri. bioRxiv.

**Appendix**

Table 1: Carbohydrate Metabolism RNAi Gene Targets

List of annotated genes in glycolysis (*HK*, *Aldolase*, *Enolase*, *PYK*), gluconeogenesis (*PEPCK*), and trehaloneogenesis (*TPS* and *TREH*), with their corresponding RNAi studies and references. ‡ indicates that additional genes were added, but not annotated in *D. citri*, such as *muscle protein 20* and *sucrose hydrolase*. * indicates that the *chitin synthase* gene in the chitin synthesis pathway was also annotated in *D. citri* [74].

| Genes | Organism | RNAi outcome | Reference |
|---|---|---|---|
| *Hexokinase* (*HK*) *Tc-HexA1* | *Tribolium castaneum* | *HexA1* role in glucose metabolism is essential during oogenesis and embryogenesis | Fraga A, Ribeiro L, Lobato M, et al. Glycogen and glucose metabolism are essential for early embryonic development of the red flour beetle *Tribolium castaneum*. PLoS One. 2013;8(6):e65125. Published 2013 Jun 4. doi:10.1371/journal.pone.0065125 |
| *Aldolase UAS-Aldolase-RNAi* | *Drosophila melanogaster* | Knockdown in *Drosophila* neurons and glia resulted in reduced lifespan; essential in glia for neuronal maintenance | Miller D, Hannon C and Ganetzky B. A mutation in *Drosophila* Aldolase causes temperature-sensitive paralysis, shortened lifespan, and neurodegeneration. J Neurogenet. 2012 Sep; 26(3-4): 317-327. 10.3109/01677063.2012.706346 |
| *Enolase* | *Nilaparvata lugens* | Knockdown reduced egg | Wang WX, Li KL, Chen Y, Lai FX Fu Q. 2015. Identification and Function Analysis |

| | | | |
|---|---|---|---|
| *α-enolase* | | production, offspring and hatching rate; mortality of adults was unaffected | of *enolase* Gene NlEno1 from *Nilaparvata lugens* (Stål) (Hemiptera:Delphacidae). J Insect Sci. 15(1):66. 10.1093/jisesa/iev046 |
| *Pyruvate kinase* (*PYK*) *NlPYK* | *Nilaparvata lugens* | RNAi treatment including triazophos and *dsNlPYK* led to reduced ovarian protein content, ovarian and fat body soluble sugar contents, and fecundity | Ge LQ, Huang B, Li X, Gu HT, Zheng S, Zhou Z, Miao H, Wu JC. Silencing pyruvate kinase (NlPYK) leads to reduced fecundity in brown planthoppers, *Nilaparvata lugens* (Stål) (Hemiptera: Delphacidae). Arch Insect Biochem Physiol. 2017 Dec;96(4). doi: 10.1002/arch.21429. Epub 2017 Nov 7. |
| *Phosphoenolpyruvate carboxykinase* (*PEPCK*) | *Drosophila melanogaster* | Knockdown of two *PEPCK* mutant isoforms led to reduced circulating glycerol levels and reduced triglyceride levels in *pepck1* mutant flies | Bartok O, Teesalu M, Ashwall-Fluss R, Pandey V, Hanan M, Rovenko BM, Poukkula M, Havula E, Moussaieff A, Vodala S et al. 2015. The transcription factor Cabut coordinates energy metabolism and the circadian clock in response to sugar sensing. EMBO J. 34(11):1538-1553. doi: 10.15252/embj.201591385. |
| *Trehalose-6-Phosphate Synthase* (*TPS*) | *Diaphorina citri* | Knockdown of the *Trehalose- 6-Phosphate Synthase* Gene Using RNA Interference Inhibits Synthesis of Trehalose and Increases Lethality Rate in Asian Citrus Psyllid | Liu, X., Zou, Z., Zhang, C., Liu, X., Wang, J., Xin, T., Xia, B. 2020. Knockdown of the Trehalose- 6-Phosphate Synthase Gene Using RNA Interference Inhibits Synthesis of Trehalose and Increases Lethality Rate in Asian Citrus Psyllid, *Diaphorina citri* (Hemiptera: Psyllidae). Insects 11: 605; doi:10.3390/insects11090605 |
| *Trehalose phosphate synthase* (*TPS*) *NlTPS* | *Nilaparvata lugens* | Feeding *N. lugens* larvae with *NlTPS* dsRNA led to disrupted expression and lethality | Chen J, Zhang D, Yao Q, Zhang J, Dong X, Tian H, Chen J, and Zhang W. 2010. Feeding-based RNA interference of a *trehalose phosphate synthase* gene in the brown planthopper, *Nilaparvata lugens*. Insect Mol. Biol. 19:777-862010 |
| *Trehalose-6-phosphate synthases* | *Nilaparvata lugens* | | Yang, M.M., Zhao, L.N., Shen, Q.D., Xie, G.Q., Wang, S.G. and Tang, B. (2017) Knockdown of two trehalose-6-phosphate synthases severely affects chitin metabolism gene expression in the brown planthopper *Nilaparvata lugens*. Pest |

| | | | |
|---|---|---|---|
| | | | Management Sciences, 73, 206-216. |
| *chitin synthase** | *Diaphorina citri* | Silencing of the chitin synthase gene is lethal to the Asian citrus psyllid | Lu, Z.J., Huang, Y.L., Yu, H.Z., Li, N.Y., Xie, Y.X., Zhang, Q et al. (2019) Silencing of the chitin synthase gene is lethal to the Asian citrus psyllid, *Diaphorina citri*. International Journal of Molecular Sciences, 20:3734. |
| five *trehalase* genes | *Tribolium castaneum* | regulates the gene expression of the chitin biosynthesis pathway | Tang, B., Wei, P., Zhao, L.N., Shi, Z.K., Shen, Q.D., Yang, M.M. et al. (2016) Knockdown of five trehalase genes using RNA interference regulates the gene expression of the chitin biosynthesis pathway in *Tribolium castaneum*. BMC Genomics, 16, 67. |
| *trehalase genes* (*TRE*) | *Nilaparvata lugens* | wing bud chitin metabolism and its development | Zhang, L., Qiu, L.Y., Yang, H.L., Wang, H.J., Zhou, M. and Wang, S.G. (2017) Study on the effect of wing bud chitin metabolism and its developmental network genes in the brown planthopper, *Nilaparvata lugens*, by knockdown of *TRE* gene. Frontiers in Physiology, 8, 750. |
| *trehalase* | *Nilaparvata lugens* | regulating the chitin metabolism pathway | Zhao, L.N., Yang, M.M., Shen, Q.D., Liu, X.J., Shi, Z.K. and Wang, S.G. (2016) Functional characterization of three trehalase genes regulating the chitin metabolism pathway in rice brown planthopper using RNA interference. Scientific Reports, 6, 27841 |

| | | | |
|---|---|---|---|
| *Muscle protein 20*‡ | *Diaphorina citri* | increases mortality to the Asian citrus psyllid, | Yu, X.D., Gowda, S. and Killiny, N. (2017) Double-stranded RNA delivery through soaking mediates silencing of the *muscle protein 20* and increases mortality to the Asian citrus psyllid, Diaphorina citri. Pest Management Science, 73, 1846-1853 |
| *Sucrose hydrolase*‡ | *Diaphorina citri* | Causes nymph mortality and disturbs adult osmotic homepstasis | Santos-Ortega, Y. and Killiny, N. (2018) Silencing of sucrose hydrolase causes nymph mortality and disturbs adult osmotic homepstasis in *Diaphorina citri* (Hemiptera: Liviidae). Insect Biochemistry and Molecular Biology, 101: 131–143. |

Table 2: Evidence Table

| **GENE** | **Identifier** | **MCOT** | ***de novo* transcripts** | **Iso - Seq** | **RNA-Seq** | **Ortholog** |
|---|---|---|---|---|---|---|
| GLYCOLYSIS | | | | | | |
| *Hexokinase type 2-1* | Dcitr03g04910.2.1 | x | x | x | x | |
| *Hexokinase type 2-2* | Dcitr03g19430.1.1 | x | x | x | x | x |
| *Hexokinase type 2-3* | Dcitr06g14200.1.1 | x | | x | x | |
| *Phosphoglucose isomerase* | Dcitr00g06460.1.1 | | x | x | x | x |
| *Glucose-6-phosphate 1-epimerase** | Dcitr13g02890.1.1 | x | x | x | x | |
| *ATP Dependent 6-Phosphofructokinase RA* | Dcitr01g16570.1.1 | x | x | x | x | x |
| *ATP Dependent 6-Phosphofructokinase RB* | Dcitr01g16570.1.2 | x | x | x | x | x |
| *ATP Dependent 6-Phosphofructokinase RC* | Dcitr01g16570.1.3 | x | x | x | x | x |

| | | | | | | |
|---|---|---|---|---|---|---|
| *Fructose-bisphosphate aldolase 1* | Dcitr04g02510.1.1 | x | x | x | x | x |
| *Fructose-bisphosphate aldolase 2* | Dcitr11g09140.1.1 | x | x | x | x | |
| *Triosephosphate isomerase* | Dcitr10g08030.1.1 | x | x | x | x | x |
| *Glyceraldehyde 3-phosphate dehydrogenase-like 1* | Dcitr10g11030.1.1 | x | | x | x | x |
| *Glyceraldehyde 3-phosphate dehydrogenase-like 2* | Dcitr01g03200.1.1 | | | x | x | |
| *Phosphoglycerate kinase* | Dcitr00g01740.1.1 | | | x | x | x |
| *Phosphoglycerate mutase 1* | Dcitr03g11640.1.1 | x | x | | x | |
| *Phosphoglycerate mutase 2* | Dcitr03g17850.1.1 | | | x | x | x |
| *Enolase* | Dcitr02g07600.1.1 | | | x | x | x |
| *Pyruvate kinase-like 1* | Dcitr07g06140.1.1 | x | x | x | x | x |
| *Pyruvate kinase-like 2* | Dcitr01g11190.1.1 | x | x | x | x | |
| *Phosphoglucomutase 1* | Dcitr05g09820.1.1 | x | | x | x | |
| *Phosphoglucomutase 2* | Dcitr02g10730.1.1 | | | x | x | x |

| GLUCONEOGENESIS | Identifier | MCOT | *de novo* transcripts | Iso-Seq | RNA-Seq | Ortholog |
|---|---|---|---|---|---|---|
| *Pyruvate carboxylase* | Dcitr08g01610.1.1 | x | x | x | x | x |
| *Phosphoenolpyruvate carboxykinase 1* | Dcitr05g10240.1.1 | x | x | x | x | |
| *Phosphoenolpyruvate carboxykinase 2* | Dcitr08g02760.1.1 | x | | x | x | x |
| *Aldose 1-epimerase 1** | Dcitr04g09830.1.1 | x | | x | x | x |
| *Aldose 1-epimerase 2** | Dcitr06g04430.1.1 | | | x | x | |
| *Fructose-1,6-bisphosphatase* | Dcitr11g08070.1.1 | | x | | x | x |

| TREHALONEOGENESIS | Identifier | MCOT | *de novo* transcripts | Iso-Seq | RNA-Seq | Ortholog |
|---|---|---|---|---|---|---|
| *Trehalose-6-phosphate synthase 1* (*TPS 1*) | Dcitr02g17550.1.1 | x | | x | x | |
| *Trehalose-6-phosphate synthase 2* (*TPS 2*) | Dcitr01g19625.1.2 | x | x | x | x | |
| *Trehalase 1A* (*TREH-1A*) *Isoform A* | Dcitr07g04030.1.1 | x | x | x | x | |
| *Trehalase 1B* (*TREH-1B*) *Isoform B* | Dcitr07g07175.1.2 | x | x | x | x | |
| *Trehalase 2* (*TREH-2*) | Dcitr08g09220.1.1 | x | x | | x | |
| *Trehalose transporter 1* (*TRET-1*) *Isoform* (*TRET-1A*) | Dcitr01g17710.1.1 | | x | x | x | |
| *Trehalose transporter 1* (*TRET-1*) *Isoform* (*TRET-1B*) | Dcitr01g17715.1.2 | x | x | x | x | |
| *Trehalose transporter 2* (*TRET-2*) *Isoform* (*TRET-2A*) | Dcitr00g03240.1.1 | x | x | x | x | |
| *Trehalose transporter 2* (*TRET-2*) *Isoform* (*TRET-2B*) | Dcitr09g02300.1.2 | x | x | x | x | |
| *Trehalose transporter 2* (*TRET-2*) *Isoform* (*TRET-2C*) | Dcitr09g02310.1.3 | | | x | x | |
| *Glucose transporter* (*GLUT 1*) | Dcitr05g13950.1.1 | x | x | x | x | x |

List of annotated *D. citri* models along with their evidence tracks. Each manually annotated gene in glycolysis, gluconeogenesis, and trehaloneogenesis associated with a *D. citri* identifier shows supporting evidence used in the curation of the gene model [42]. Evidence tracks are as follows: RNA-Seq, long-read Iso-Seq, MCOT, *de novo* assembled transcripts and orthologous proteins. A gene marked with an “x” within the table indicates that the gene model is supported by the evidence track. A gene followed with an “*” indicates that it is involved in both glycolysis and gluconeogenesis.

**Table 3:** Heat map values in Transcripts per million (TPM); glycolysis energy investment phase

| Gene Name | *Hexokinase type 2-2* | *Hexokinase type 2-3* | *Phosphoglucose isomerase* | *Glucose-6-phosphate 1-epimerase* | *ATP Dependent 6-Phosphofructokinase* | *Fructose-bisphosphate aldolase 1* | *Fructose-bisphosphate aldolase 2* | *Triosephosphate isomerase* | *Phosphoglucomutase 1* | *Phosphoglucomutase 2* |
|---|---|---|---|---|---|---|---|---|---|---|
| Dcitri ID | Dcitr03g19430.1.1 | Dcitr06g14200.1.1 | Dcitr00g06460.1.1 | Dcitr13g02890.1.1 | Dcitr01g16570.1.1 | Dcitr04g02510.1.1 | Dcitr11g09140.1.1 | Dcitr10g08030.1.1 | Dcitr05g09820.1.1 | Dcitr02g10730.1.1 |
| Egg C. mac *C*Las- Whole body | 25.15 | 97.85 | 171.89 | 57.81 | 49.51 | 2.04 | 0 | 108.16 | 97.13 | 14.23 |
| Nymph C. med *C*Las+ Low inf Whole body | 59.72 | 217.92 | 121.32 | 31.17 | 104.71 | 9.81 | 37.41 | 176.97 | 241.75 | 18.09 |
| Nymph C. sin *C*Las+ High inf Whole body | 59.13 | 221.91 | 121.14 | 27.34 | 100.34 | 11.34 | 0 | 193.88 | 268.3 | 19.07 |
| Nymph C. sin *C*Las- Whole body | 47.64 | 188.31 | 119.91 | 25.73 | 94.65 | 4.68 | 0 | 156.66 | 178.92 | 19.17 |
| Nymph C. macrophylla *C*Las- Whole body | 158.14 | 127.16 | 101.02 | 34.15 | 87.25 | 6.24 | 130.71 | 76.46 | 130.6 | 19.08 |
| Nymph Citrus *C*Las- Whole body | 176.73 | 200.69 | 65.57 | 10.78 | 49 | 1.09 | 168.55 | 52.78 | 125.67 | 11.6 |
| Nymph Citrus *C*Las+ Whole body | 24.23 | 217.32 | 165.09 | 14.21 | 38.68 | 7.33 | 0 | 176.33 | 314.64 | 11.81 |
| Adult C. med *C*Las- Gut | 135.7 | 1060.82 | 198.23 | 110.24 | 69.2 | 7.49 | 0 | 142.44 | 382.16 | 17.57 |

| | | | | | | | | | | |
|---|---|---|---|---|---|---|---|---|---|---|
| Adult C. med *C*Las+ Gut | 129.79 | 723.37 | 226.85 | 102.83 | 65.23 | 3.14 | 33.19 | 163.82 | 363.07 | 21.65 |
| Adult C. med *C*Las+ High inf Whole body | 112.65 | 253.43 | 174.06 | 25.64 | 199.15 | 88.02 | 0 | 227.01 | 212.84 | 35.33 |
| Adult C. med *C*Las+ Low inf Whole body | 75.09 | 283.4 | 127.99 | 31.58 | 100.45 | 105.86 | 34.66 | 158.69 | 185.24 | 43.71 |
| Adult C. med *C*Las- Whole body | 109.36 | 248.57 | 168.6 | 29.92 | 189.3 | 71.83 | 0 | 233.78 | 173.95 | 32.65 |
| Adult C. mac *C*Las- Whole body | 68.99 | 335.31 | 220.29 | 41.38 | 121.54 | 175.37 | 389.34 | 143.76 | 240.32 | 35.39 |
| Adult Citrus *C*Las- Whole body | 144.65 | 470 | 114.94 | 29.63 | 65.96 | 163.77 | 320.52 | 129.96 | 213.64 | 21.88 |
| Adult Citrus *C*Las+ Whole body | 112.61 | 369.54 | 204.14 | 22.34 | 70.46 | 56.74 | 0 | 164.13 | 162.25 | 31.27 |
| Adult Citrus *C*Las- midgut | 126.12 | 816.14 | 345.75 | 43.78 | 106.6 | 3.88 | 480.25 | 178.47 | 370.54 | 9.04 |
| Adult Citrus *C*Las+ midgut | 68.92 | 1214.13 | 293.63 | 41.99 | 78.21 | 8.6 | 322.57 | 200.09 | 309.96 | 11.07 |
| Adult C. ret *C*Las- Female abdomen | 117.53 | 270.82 | 328.46 | 4.18 | 67.72 | 0.91 | 639.1 | 174.79 | 184.51 | 49.43 |
| Adult C. ret *C*Las- Female antennae | 31.32 | 268.93 | 341.64 | 7.02 | 44.09 | 3.19 | 502.23 | 269.09 | 110.49 | 15.66 |
| Adult C. ret *C*Las- Female head | 54.9 | 396.04 | 398.25 | 16.84 | 68.99 | 0 | 838.36 | 293.04 | 123.87 | 12.75 |
| Adult C. ret *C*Las- Female leg | 52.67 | 124.32 | 379.99 | 9.34 | 60.59 | 0 | 742.14 | 454.38 | 138.65 | 14.02 |

| | | | | | | | | | | |
|---|---|---|---|---|---|---|---|---|---|---|
| Adult C. ret *C*Las-Female terminal abdomen | 26.34 | 163.63 | 297.31 | 2.43 | 31.68 | 1.02 | 248.39 | 335.32 | 112.84 | 11.2 |
| Adult C. ret *C*Las-Female thorax | 176.24 | 170.66 | 783.82 | 9.36 | 634.34 | 0.67 | 1853.95 | 610.79 | 228.8 | 6.34 |
| Adult C. ret *C*Las-Male abdomen | 127.94 | 314.79 | 269.51 | 17.09 | 66.31 | 110.94 | 644.54 | 167.03 | 144.26 | 37.53 |
| Adult C. ret *C*Las-Male antennae | 49.54 | 221.2 | 323.43 | 15.46 | 52.72 | 19.77 | 459.43 | 221.47 | 107.6 | 22.6 |
| Adult C. ret *C*Las-Male head | 57.63 | 436.71 | 383.61 | 17.88 | 88.31 | 1.89 | 1021.53 | 290.42 | 146.25 | 13.7 |
| Adult C. ret *C*Las-Male leg | 123.53 | 216.12 | 402.16 | 13.23 | 102.63 | 41.16 | 1200.77 | 449.2 | 133.17 | 12.53 |
| Adult C. ret *C*Las-Male terminal abdomen | 56.55 | 178.64 | 212.71 | 10.84 | 41.28 | 45.26 | 257.23 | 146.16 | 83.44 | 12.96 |
| Adult C. ret *C*Las-Male thorax | 164.62 | 214.79 | 772.34 | 12.94 | 594.73 | 8.14 | 1853.38 | 559.97 | 247.77 | 13.9 |
| Adult C. ret *C*Las-Female antennae [#] | 178.95 | 426.84 | 316.22 | 28.42 | 141.51 | 0 | 699.25 | 245.8 | 185.45 | 22.26 |
| Adult C. ret *C*Las-Female terminal abdomen [#] | 121.72 | 474.78 | 245.24 | 10.41 | 67.37 | 1.65 | 367.9 | 219.89 | 152.34 | 27.72 |
| Adult C. ret *C*Las-Male antennae [#] | 151.61 | 406.33 | 301.78 | 44.06 | 154.72 | 12.67 | 780.47 | 241.75 | 171.32 | 25.82 |
| Adult C. ret *C*Las-Male terminal abdomen [#] | 189.97 | 251 | 158.74 | 22.41 | 73.91 | 131.44 | 441.93 | 139.27 | 113.39 | 18.07 |

Comparison of RNA-Seq datasets of genes involved in the energy investment phase of glycolysis. Heatmap shows results from *D. citri* reared on various citrus varieties, both infected and uninfected with *C*Las. Expression values were collected from Citrus Greening expression network [36]. Data in the heatmap shows transcripts per million scaled by row. RNA-seq data is available from NCBI Bioproject's PRJNA609978 and PRJNA448935 and published data sets [53].

**Table 4:** Heat map values in Transcripts per million (TPM); glycolysis energy production phase

| Gene Name | *Glyceraldehyde 3-phosphate dehydrogenase-like 1* | *Glyceraldehyde 3-phosphate dehydrogenase-like 2* | *Phosphoglycerate kinase* | *Phosphoglycerate mutase 1* | *Phosphoglycerate mutase 2* | *Enolase* | *Pyruvate kinase-like 1* | *Pyruvate kinase-like 2* |
|---|---|---|---|---|---|---|---|---|
| Dcitri ID | Dcitr10g11030.1.1 | Dcitr01g03200.1.1 | Dcitr00g01740.1.1 | Dcitr03g11640.1.1 | Dcitr03g17850.1.1 | Dcitr02g07600.1.1 | Dcitr07g06140.1.1 | Dcitr01g11190.1.1 |
| Egg C. mac *C*Las-Whole body | 0.59 | 182.74 | 120.15 | 27.68 | 48.76 | 157.41 | 275.06 | 0.11 |
| Nymph C. med *C*Las+ Low inf Whole body | 11.8 | 1281.17 | 119.41 | 21.05 | 211.62 | 396.15 | 677.59 | 3.15 |
| Nymph C. sin *C*Las+ High inf Whole body | 12.09 | 1199.18 | 117.22 | 15.68 | 207.93 | 346.1 | 663.43 | 3.59 |
| Nymph C. sin *C*Las-Whole body | 7.97 | 565.4 | 126.37 | 21.73 | 155.93 | 412.17 | 601.46 | 2.09 |
| Nymph C. macrophylla *C*Las- | 6.19 | 955.29 | 71.65 | 13.57 | 81.84 | 395.72 | 706.05 | 2.28 |

| | | | | | | | | |
|---|---|---|---|---|---|---|---|---|
| Whole body | | | | | | | | |
| Nymph Citrus *C*Las- Whole body | 0.24 | 555.48 | 61.87 | 8.95 | 36.78 | 394.19 | 306.25 | 0.5 |
| Nymph Citrus *C*Las+ Whole body | 12.34 | 207.28 | 157.88 | 4.67 | 93.34 | 383.17 | 247.07 | 4.31 |
| Adult C. med *C*Las- Gut | 3.04 | 633.03 | 141.87 | 77.89 | 131.03 | 223.07 | 1126.6 | 1.39 |
| Adult C. med *C*Las+ Gut | 0.88 | 389.71 | 173.66 | 69.12 | 141.87 | 336.91 | 1018.83 | 0.56 |
| Adult C. med *C*Las+ High inf Whole body | 43.76 | 1564.75 | 154.15 | 32.65 | 237.17 | 550.47 | 1123.72 | 19.42 |
| Adult C. med *C*Las+ Low inf Whole body | 52.74 | 1008.06 | 111.12 | 16.79 | 166.46 | 441.1 | 699.31 | 20.54 |
| Adult C. med *C*Las- Whole body | 33.18 | 2150.93 | 139.84 | 29.07 | 349.47 | 588.11 | 1225.39 | 13.05 |
| Adult C. mac *C*Las- Whole body | 73.76 | 536.23 | 134.28 | 19.04 | 105.47 | 504.39 | 691.87 | 29.37 |
| Adult Citrus *C*Las- Whole body | 99.93 | 718.64 | 142.36 | 26.28 | 142.7 | 770.88 | 1264.01 | 36.66 |
| Adult Citrus *C*Las+ Whole body | 63.11 | 636.58 | 174.11 | 11.06 | 111.02 | 295.73 | 550.94 | 25.12 |
| Adult Citrus *C*Las- midgut | 2.72 | 652.67 | 204.2 | 140.66 | 112.2 | 200.34 | 1230.3 | 1.88 |
| Adult Citrus *C*Las+ midgut | 15.36 | 529.27 | 202.19 | 80.52 | 112.27 | 222.02 | 948.04 | 3.6 |
| Adult C. ret *C*Las- Female abdomen | 0.97 | 598.04 | 173.24 | 10.07 | 92.03 | 285.51 | 405.45 | 1.03 |

| | | | | | | | | |
|---|---|---|---|---|---|---|---|---|
| Adult C. ret *C*Las-Female antennae | 5.69 | 528.62 | 188.31 | 1.72 | 124.44 | 261.31 | 212.55 | 0.86 |
| Adult C. ret *C*Las-Female head | 0 | 605.38 | 250.95 | 5.34 | 132.82 | 290.28 | 282.56 | 0.18 |
| Adult C. ret *C*Las-Female leg | 0 | 510.04 | 225.49 | 8.24 | 156.33 | 264.93 | 207.95 | 0.18 |
| Adult C. ret *C*Las-Female terminal abdomen | 2.54 | 251.14 | 234.36 | 1.6 | 166.49 | 142.35 | 125.6 | 0.71 |
| Adult C. ret *C*Las-Female thorax | 0.95 | 2197.87 | 600.77 | 57.09 | 362.69 | 1060.66 | 2027.77 | 0.44 |
| Adult C. ret *C*Las-Male abdomen | 98.38 | 524.78 | 140.98 | 23.59 | 90.65 | 207.4 | 368.01 | 26.66 |
| Adult C. ret *C*Las-Male antennae | 44.77 | 487.63 | 149.7 | 10.21 | 113.27 | 253.49 | 237.84 | 5.95 |
| Adult C. ret *C*Las-Male head | 0.35 | 688.3 | 240.81 | 5.2 | 131.1 | 319.34 | 343.32 | 0.34 |
| Adult C. ret *C*Las-Male leg | 27.5 | 814.67 | 254.57 | 20.46 | 182.69 | 383.3 | 425.54 | 10.09 |
| Adult C. ret *C*Las-Male terminal abdomen | 59.56 | 300.01 | 121.77 | 6.45 | 79.42 | 128.97 | 130.17 | 16.15 |
| Adult C. ret *C*Las-Male thorax | 5.91 | 2280.77 | 534.62 | 67.48 | 357.02 | 949.95 | 1993.44 | 1.94 |
| Adult C. ret *C*Las-Female antennae [#] | 0 | 690.48 | 231.99 | 12.94 | 127.8 | 342.94 | 484.68 | 0.54 |
| Adult C. ret *C*Las-Female terminal | 4.21 | 572.98 | 212.06 | 11.09 | 101.21 | 252.78 | 378.03 | 0.55 |

| | | | | | | | | |
|---|---|---|---|---|---|---|---|---|
| abdomen [#] | | | | | | | | |
| Adult C. ret *C*Las- Male antennae [#] | 15.6 | 580.98 | 196.65 | 13.25 | 126.54 | 308.74 | 467.92 | 5.44 |
| Adult C. ret *C*Las- Male terminal abdomen [#] | 132.64 | 486.15 | 130.26 | 15.15 | 81.52 | 210.65 | 229.51 | 43.72 |

Comparison of RNA-Seq datasets of genes involved in the energy production phase of glycolysis. Heatmap shows results from *D. citri* reared on various citrus varieties, both infected and uninfected with *C*Las. Expression values were collected from Citrus Greening expression network [36]. Data in the heatmap shows transcripts per million scaled by row. RNA-seq data is available from NCBI Bioproject's PRJNA609978 and PRJNA448935 and published data sets [53].

**Table 5:** Heat map values in Transcripts per million (TPM); Gluconeogenesis

| Gene Name | *Pyruvate carboxylase* | *Phosphoenolpyruvate carboxykinase 1* | *Phosphoenolpyruvate carboxykinase 2* | *Aldose 1-epimerase 1* | *Aldose 1-epimerase 2* | *Fructose-1,6-bisphosphatase* |
|---|---|---|---|---|---|---|
| Dcitri ID | Dcitr08g01610.1.1 | Dcitr05g10240.1.1 | Dcitr08g02760.1.1 | Dcitr04g09830.1.1 | Dcitr06g04430.1.1 | Dcitr11g08070.1.1 |
| Egg C. mac *C*Las- Whole body | 144.93 | 221.31 | 47.96 | 20.23 | 7.67 | 113.26 |
| Nymph C. med *C*Las+ Low inf Whole body | 79.91 | 101.91 | 306.67 | 21.94 | 39.81 | 44.02 |

| | | | | | | |
|---|---|---|---|---|---|---|
| Nymph C. sin *C*Las+ High inf Whole body | 96.3 | 125.86 | 240.3 | 24.7 | 35.52 | 44.51 |
| Nymph C. sin *C*Las- Whole body | 87.05 | 98.92 | 383.51 | 20.29 | 20.74 | 50.06 |
| Nymph C. macrophylla *C*Las- Whole body | 116.16 | 21.02 | 339.41 | 16.12 | 21.96 | 14.5 |
| Nymph Citrus *C*Las- Whole body | 92.52 | 71.12 | 269.45 | 20.42 | 2.87 | 29.17 |
| Nymph Citrus *C*Las+ Whole body | 78.49 | 20.64 | 492.1 | 32.65 | 3.89 | 6.13 |
| Adult C. med *C*Las- Gut | 80.51 | 57.03 | 11.38 | 68.49 | 2.55 | 1.69 |
| Adult C. med *C*Las+ Gut | 78.76 | 40.46 | 16.65 | 85.93 | 4.77 | 2.97 |
| Adult C. med *C*Las+ High inf Whole body | 183.84 | 659.9 | 296.96 | 34.19 | 10.18 | 66.67 |
| Adult C. med *C*Las+ Low inf Whole body | 161.08 | 161.41 | 318.92 | 30.92 | 16.24 | 67.56 |
| Adult C. med *C*Las- Whole body | 161.54 | 263.13 | 322.04 | 29.55 | 17.18 | 31.32 |
| Adult C. mac *C*Las- Whole body | 266.52 | 327.57 | 297.26 | 35.88 | 14.47 | 85.57 |
| Adult Citrus *C*Las- Whole body | 349.71 | 134.56 | 574.32 | 41.83 | 2.42 | 57.79 |
| Adult Citrus *C*Las+ Whole body | 235.21 | 279.83 | 226.97 | 44.54 | 13.74 | 29.7 |
| Adult Citrus *C*Las- midgut | 85.59 | 96.92 | 31.96 | 55.12 | 8.92 | 1.87 |

| | | | | | | |
|---|---|---|---|---|---|---|
| Adult Citrus *C*Las+ midgut | 64.57 | 181.37 | 30.8 | 58.9 | 8.25 | 5.93 |
| Adult C. ret *C*Las- Female abdomen | 317.7 | 587.15 | 341.26 | 38.76 | 16.23 | 36.79 |
| Adult C. ret *C*Las- Female antennae | 226.26 | 1211.21 | 22.2 | 10.45 | 8.31 | 14.35 |
| Adult C. ret *C*Las- Female head | 298.32 | 2236.36 | 1.63 | 12.67 | 6.71 | 19.49 |
| Adult C. ret *C*Las- Female leg | 198.12 | 1020.26 | 31.11 | 18.75 | 6.06 | 19.5 |
| Adult C. ret *C*Las- Female terminal abdomen | 158.35 | 461.64 | 21.03 | 16.33 | 29.08 | 9.3 |
| Adult C. ret *C*Las- Female thorax | 442.95 | 2219.87 | 2.39 | 8.96 | 2.5 | 22.6 |
| Adult C. ret *C*Las- Male abdomen | 228.67 | 707.08 | 178.74 | 26.38 | 26.63 | 15.01 |
| Adult C. ret *C*Las- Male antennae | 177.52 | 1137.73 | 27.31 | 7.7 | 10.69 | 15.69 |
| Adult C. ret *C*Las- Male head | 290.56 | 2154.94 | 0.71 | 10.6 | 6.24 | 18.69 |
| Adult C. ret *C*Las- Male leg | 207.16 | 1560.47 | 20.49 | 16.42 | 2.53 | 19.39 |
| Adult C. ret *C*Las- Male terminal abdomen | 105.46 | 464.59 | 3.83 | 18.17 | 39.16 | 11.48 |
| Adult C. ret *C*Las- Male thorax | 412.38 | 1749.69 | 1.95 | 13.12 | 1.3 | 21.33 |
| Adult C. ret *C*Las- Female antennae [#] | 440.48 | 3262.92 | 61.4 | 20.92 | 8 | 67.78 |

| | | | | | | |
|---|---|---|---|---|---|---|
| Adult C. ret *C*Las- Female terminal abdomen [#] | 277.06 | 1317 | 380.03 | 36.08 | 40.76 | 38.22 |
| Adult C. ret *C*Las- Male antennae [#] | 351.01 | 2753.66 | 3.69 | 14.39 | 5.27 | 43.66 |
| Adult C. ret *C*Las- Male terminal abdomen [#] | 161.67 | 1163.15 | 72.59 | 21.28 | 59.17 | 26.02 |

Comparison of RNA-Seq datasets of genes involved in gluconeogenesis. Heatmap shows results from *D. citri* reared on various citrus varieties, both infected and uninfected with *C*Las. Expression values were collected from Citrus Greening expression network [36]. Data in the heatmap shows transcripts per million scaled by row. RNA-seq data is available from NCBI Bioproject's PRJNA609978 and PRJNA448935 and published data sets [53].

**Table 6:** Heat map values in Transcripts per million (TPM); Trehaloneogenesis

| Gene Name | *Trehalose-6-phosphate synthase 1* (*TPS 1*) | *Trehalase 1A* (*TREH-1A*) *Isoform A* | *Trehalase 2* (*TREH-2*) | *Trehalose transporter 1* (*TRET-1*) *Isoform* (*TRET-1A*) | *Trehalose transporter 2* (*TRET-2*) *Isoform* (*TRET-2A*) | *Glucose transporter* (*GLUT 1*) |
|---|---|---|---|---|---|---|
| Dcitri ID | Dcitr02g17550.1.1 | Dcitr07g04030.1.1 | Dcitr08g09220.1.1 | Dcitr01g17710.1.1 | Dcitr00g03240.1.1 | Dcitr05g13950.1.1 |
| Egg C. mac *C*Las- Whole body | 26.15 | 9.71 | 11.28 | 26.72 | 3.83 | 41.58 |
| Nymph C. med *C*Las+ Low inf Whole body | 38.11 | 6.84 | 22.35 | 86.73 | 8.01 | 27.03 |
| Nymph C. sin *C*Las+ | 22.73 | 6.3 | 30.1 | 141.06 | 16.04 | 23.11 |

| | | | | | | |
|---|---|---|---|---|---|---|
| High inf Whole body | | | | | | |
| Nymph C. sin *C*Las- Whole body | 13.79 | 5.15 | 20.03 | 64.45 | 3.02 | 27.56 |
| Nymph C. macrophylla *C*Las- Whole body | 23.76 | 7.57 | 44.98 | 173.44 | 11.95 | 29.79 |
| Nymph Citrus *C*Las- Whole body | 46.52 | 0.71 | 17.21 | 186.32 | 7.76 | 23.91 |
| Nymph Citrus *C*Las+ Whole body | 23.03 | 1.94 | 12.82 | 110.14 | 17.34 | 10.14 |
| Adult C. med *C*Las- Gut | 150.06 | 86.45 | 4.5 | 1119.48 | 0.37 | 15.89 |
| Adult C. med *C*Las+ Gut | 119.85 | 34.17 | 4.37 | 1188.92 | 0.36 | 27.06 |
| Adult C. med *C*Las+ High inf Whole body | 64.44 | 15.27 | 34.14 | 152.09 | 13.2 | 30.87 |
| Adult C. med *C*Las+ Low inf Whole body | 50.32 | 20.36 | 32.9 | 147.25 | 9.5 | 29.03 |
| Adult C. med *C*Las- Whole body | 48.37 | 8.61 | 29.59 | 181.68 | 8.5 | 19.67 |
| Adult C. mac *C*Las- Whole body | 8.54 | 21.23 | 29.65 | 121.36 | 16.82 | 26.31 |
| Adult Citrus *C*Las- Whole body | 125.13 | 12.55 | 36.65 | 256.62 | 21.31 | 23.38 |
| Adult Citrus *C*Las+ Whole body | 52.09 | 12.83 | 18.27 | 144.39 | 21.35 | 21.99 |
| Adult Citrus *C*Las- midgut | 376.6 | 43.85 | 5.89 | 270.16 | 1.1 | 28 |

| | | | | | | |
|---|---|---|---|---|---|---|
| Adult Citrus *C*Las+ midgut | 444.12 | 66.12 | 4.34 | 77.36 | 0.76 | 21.19 |
| Adult C. ret *C*Las- Female abdomen | 113.01 | 14.52 | 32.16 | 264.69 | 72.63 | 22.83 |
| Adult C. ret *C*Las- Female antennae | 34.25 | 1.63 | 33.31 | 31.37 | 45.72 | 16.67 |
| Adult C. ret *C*Las- Female head | 39.4 | 1.2 | 38.89 | 30.75 | 77.48 | 16.92 |
| Adult C. ret *C*Las- Female leg | 25.8 | 2.11 | 30.58 | 30.4 | 33.63 | 9.5 |
| Adult C. ret *C*Las- Female terminal abdomen | 12.03 | 2.26 | 21.75 | 18.55 | 23.16 | 6.77 |
| Adult C. ret *C*Las- Female thorax | 70.13 | 5.65 | 52.41 | 52.3 | 63.82 | 21.66 |
| Adult C. ret *C*Las- Male abdomen | 145 | 16.45 | 30.95 | 236.71 | 97.75 | 20.8 |
| Adult C. ret *C*Las- Male antennae | 46.73 | 2.62 | 38.15 | 67.03 | 40.57 | 19.4 |
| Adult C. ret *C*Las- Male head | 41.65 | 0.74 | 33.59 | 32.14 | 65.72 | 20.93 |
| Adult C. ret *C*Las- Male leg | 59 | 4.63 | 37.99 | 65.81 | 50.06 | 22.12 |
| Adult C. ret *C*Las- Male terminal abdomen | 31.18 | 1.69 | 17.77 | 65.32 | 12.56 | 12.67 |
| Adult C. ret *C*Las- Male thorax | 69.26 | 6.39 | 46.63 | 57.57 | 65.55 | 19.87 |

| | | | | | | |
|---|---|---|---|---|---|---|
| Adult C. ret *C*Las-Female antennae [#] | 121.22 | 10.8 | 40.97 | 136.41 | 33.71 | 36.25 |
| Adult C. ret *C*Las-Female terminal abdomen [#] | 187.13 | 30.86 | 19.02 | 294.01 | 14.35 | 15.35 |
| Adult C. ret *C*Las- Male antennae [#] | 90.25 | 6.06 | 52.27 | 145.34 | 49.07 | 42.13 |
| Adult C. ret *C*Las- Male terminal abdomen [#] | 134.98 | 13.99 | 26.84 | 363.12 | 24.28 | 22.94 |

Comparison of RNA-Seq datasets of genes involved in trehaloneogenesis. Heatmap shows results from *D. citri* reared on various citrus varieties, both infected and uninfected with *C*Las. Expression values were collected from Citrus Greening expression network [36]. Data in the heatmap shows transcripts per million scaled by row. RNA-seq data is available from NCBI Bioproject's PRJNA609978 and PRJNA448935 and published data sets [53].